

**TRANSUCTANEOUS CYANOMETER: IMPROVEMENT OF
IOT-BASED CYANOSIS DETECTION DEVICE FOR NEWBORN
ASSESSMENT IN MEDICAL TRAINING APPLICATION**

MUHAMMAD EMIL HAZIQ BIN MOHAMMAD ALI



UNIVERSITI TEKNIKAL MALAYSIA MELAKA

**TRANSUCTANEOUS CYANOMETER: IMPROVEMENT OF
IOT-BASED CYANOSIS DETECTION DEVICE FOR
NEWBORN ASSESSMENT IN MEDICAL TRAINING
APPLICATION**

MUHAMMAD EMIL HAZIQ BIN MOHAMMAD ALI

**This report is submitted in partial fulfilment of the requirements
for the degree of Bachelor of Electronic Engineering with Honours**

**Faculty of Electronic and Computer Technology and Engineering
Universiti Teknikal Malaysia Melaka**

2024

BORANG PENGESAHAN STATUS LAPORAN
PROJEK SARJANA MUDA II

Tajuk Projek : TRANSUCTANEOUS CYANOMETER: IMPROVEMENT OF IOT-BASED CYANOSIS DETECTION DEVICE FOR NEWBORN ASSESSMENT IN MEDICAL TRAINING APPLICATION

Sesi Pengajian : 2023/2024

Saya MUHAMMAD EMIL HAZIQ BIN MOHAMMAD ALI mengaku membenarkan laporan Projek Sarjana Muda ini disimpan di Perpustakaan dengan syarat-syarat kegunaan seperti berikut:

1. Laporan adalah hakmilik Universiti Teknikal Malaysia Melaka.
2. Perpustakaan dibenarkan membuat salinan untuk tujuan pengajian sahaja.
3. Perpustakaan dibenarkan membuat salinan laporan ini sebagai bahan pertukaran antara institusi pengajian tinggi.
4. Sila tandakan (✓):

SULIT*

(Mengandungi maklumat yang berdarjah keselamatan atau kepentingan Malaysia seperti yang termaktub di dalam AKTA RAHSIA RASMI 1972)

TERHAD*

(Mengandungi maklumat terhadap yang telah ditentukan oleh organisasi/badan di mana penyelidikan dijalankan.

TIDAK TERHAD

Disahkan oleh:


(TANDATANGAN PENULIS)


(COP DAN TANDATANGAN PENYELIA)

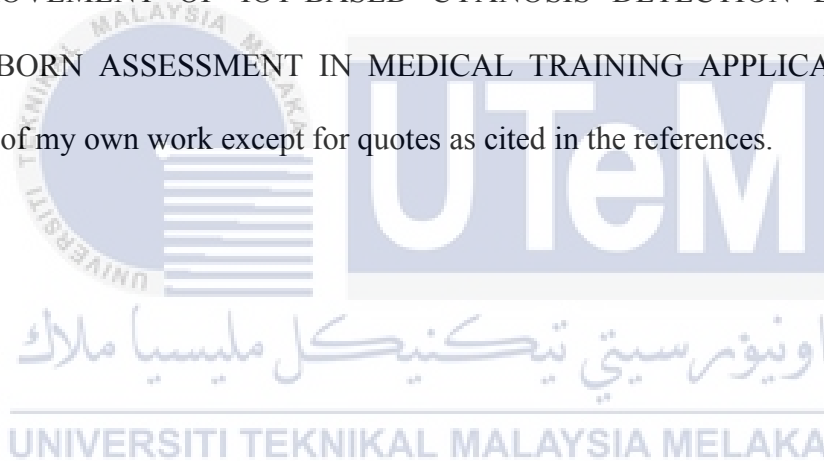
Alamat Tetap: 84, HALA RAPAT BARU 26, TAMAN TAUFIK, 31350 IPOH, PERAK

TS. DR. NUR FATIHAH BINTI AZMI
Senior Lecturer
Fakulti Teknologi dan Kejuruteraan Elektronik dan Komputer (FTKEK)
Universiti Teknikal Malaysia Melaka (UTeM)
Jalan Hang Tuah Jaya, 76100 Durian Tunggal, Melaka, Malaysia

Tarikh : 12 JANUARI 2024 Tarikh : 12 JANUARI 2024

DECLARATION

I declare that this report entitled “TRANSUCTANEOUS CYANOMETER: IMPROVEMENT OF IOT-BASED CYANOSIS DETECTION DEVICE FOR NEWBORN ASSESSMENT IN MEDICAL TRAINING APPLICATION” is the result of my own work except for quotes as cited in the references.



Signature :

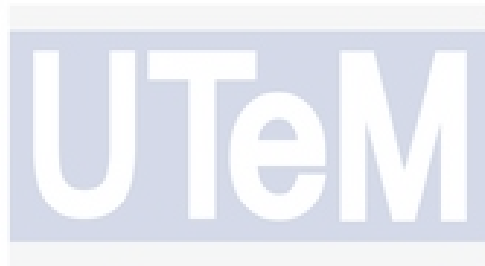
A handwritten signature in black ink, appearing to be 'Emil Haziq', is written over the dotted line of the signature field.

Author : MUHAMMAD EMIL HAZIQ BIN
MOHAMMAD ALI

Date : 12 JANUARY 2024

APPROVAL

I hereby declare that I have read this thesis and in my opinion this thesis is sufficient in terms of scope and quality for the award of Bachelor of Electronic Engineering with Honours.



اونیورسیتی تکنیکل ملیسیا ملاک
Signature : 

UNIVERSITI TEKNIKAL MALAYSIA MELAKA

Supervisor Name : TS. DR. NUR FATIHAH BINTI AZMI

Date : 12 JANUARY 2024

DEDICATION

This study is wholeheartedly dedicated for both my parents, Mohammad Ali bin Mohd Jali and Shahrizan binti Mohd Bashir, who have always supported and encouraged me in any situation. To all my beloved friends, who helped me a lot throughout the production of this project. Only God can reward all your good deeds. And finally, this dedication is specially made for the Almighty Creator, thank you for your guidance. May we all be under His protection.

اونيورسيتي تيكنيكل مليسيا ملاك
UNIVERSITI TEKNIKAL MALAYSIA MELAKA

ABSTRACT

Cyanosis is characterized by bluish discoloration of the skin, mucous membranes, and nails due to deoxygenated haemoglobin in blood near the skin's surface. It can indicate underlying medical conditions such as lung or respiratory issues, heart problems, and blood disorders in newborn infants. Therefore, immediate consultation with a medical practitioner for evaluation is essential to address any potential impact on the baby's health and well-being. While medical technology has progressed, no widely accepted method for automatically detecting and quantifying cyanotic skin color in newborns remains. To address this gap, this study proposes the development of a Transcutaneous CyanoMeter: A Non-Invasive Cyanosis Detector that utilizes RGB color values from a TCS34725 color sensor to detect and measure bluish discoloration on newborn skin, particularly around the lips, to determine cyanosis level. The goal is to establish a device that can accurately detect cyanosis in newborns in RGB space, potentially aiding new medical doctors in evaluating babies using IoT implementation, thereby making it valuable within the medical industry.

ABSTRAK

Sianosis dicirikan oleh perubahan warna kebiruan pada kulit, membran mukus, dan kuku disebabkan oleh hemoglobin yang kurang oksigen dalam darah di permukaan kulit. Ia menunjukkan bahawa terdapatnya masalah kesihatan seperti isu pernafasan, masalah jantung, dan gangguan darah pada bayi baru lahir. Oleh itu, konsultasi segera dengan pegawai perubatan untuk penilaian adalah penting untuk menangani sebarang impak yang mungkin berlaku terhadap kesihatan dan kesejahteraan bayi. Walaupun teknologi perubatan telah berkembang, masih tiada kaedah yang secara meluas diterima untuk mengesan dan mengukur secara automatik warna kulit yang sianotik pada bayi baru lahir. Bagi mengatasi masalah ini, kajian ini mencadangkan pembangunan Transcutaneous CyanoMeter: Alat Pengesan Sianosis yang menggunakan nilai warna RGB dari sensor warna TCS34725 untuk mengesan dan mengukur perubahan warna biru pada kulit bayi, khususnya di sekitar bibir, untuk menentukan tahap sianosis. Matlamatnya adalah untuk membina sebuah peranti yang dapat mengesan sianosis secara tepat dalam ruang RGB pada bayi baru lahir, dengan harapan dapat membantu doktor perubatan baru dalam menilai bayi menggunakan pelaksanaan IoT, menjadikannya bermanfaat dalam industri perubatan.

ACKNOWLEDGEMENTS

I am very thankful to Allah S.W.T for giving me the strength and determination to start and successfully complete this project. I want to thank my supervisor, Dr. Nur Fatihah binti Azmi, for her constant support and guidance throughout the process. I also appreciate the help of my friends, whose encouragement was crucial in overcoming challenges. I am grateful for the educational opportunities provided by Universiti Teknikal Malaysia, Melaka, which has helped me develop both personally and academically.

UNIVERSITI TEKNIKAL MALAYSIA MELAKA

TABLE OF CONTENTS

Declaration	
Approval	
Dedication	
Abstract	i
Abstrak	ii
Acknowledgements	iii
Table of Contents	iv
List of Figures	ix
List of Tables	xi
List of Symbols and Abbreviations	xii
CHAPTER 1 INTRODUCTION	1
1.1 Background	1
1.2 Problem Statement	2
1.3 Objectives	3
1.4 Significance of the Study	3
1.5 Scope of the Study	4

1.6	Organization of the Thesis	5
CHAPTER 2 BACKGROUND STUDY		7
2.1	Cyanosis	7
2.2	Apgar Score	9
2.3	RGB Color Space	11
2.4	Cyanosis Color Values	12
2.5	Harnessing Color Vision	14
2.6	Colorimeter in detecting colors	15
2.6.1	Summary of Colorimeter Specifications	17
2.7	Summary of the literature review	21
CHAPTER 3 METHODOLOGY		23
3.1	Flowchart	24
3.2	Prototype Design and Fabrication	25
3.2.1	3D Model Design	25
3.2.2	Fabrication	27
3.3	Circuit Components	29
3.4	Color Reference Selection	31
3.4.1	Dataset Lip Selection	31
3.4.2	RAL K7 Comparison	32
3.4.3	Practical Challenges in Lip Color Measurement	34

3.5	Color Sensor Accuracy Experiment	34
3.5.1	TCS34725 Calibration	34
3.5.2	Experimental Lighting Sources	35
3.5.3	LED (4150K) Direct Measurement	36
3.5.3.1	Measurement Approach	36
3.5.3.2	Brightness Configuration	38
3.5.4	3000K Bulb and 6500K Bulb	38
3.5.4.1	Shared Measurement Setup	38
3.5.4.2	Distance Configuration	40
3.6	IoT Implementation	40
3.7	Cyanosis RGB Threshold	42
3.8	Color Measurement and Data Acquisition	43
3.8.1	Euclidean Distance in RGB	43
3.8.2	T-test: Two-sample for Means	44
3.8.3	Pearson Correlation Coefficient	45
CHAPTER 4 RESULTS AND DISCUSSION		46
4.1	LED (4150K) Direct Measurement	46
4.1.1	RAL K7 Color Reference Comparison and Euclidean Distance	46
4.1.2	Statistical Analysis	48
4.1.3	3D Scatter Plot Graph	49

4.1.4	Pearson Correlation Coefficient	52
4.2	Bulb (3000K) Measurement	53
4.2.1	RAL K7 Color Reference Comparison and Euclidean Distance	53
4.2.2	Statistical Analysis	54
4.2.3	3D Scatter Plot Graph	55
4.2.4	Pearson Correlation Coefficient	57
4.3	Bulb (6500K) Measurement	58
4.3.1	RAL K7 Color Reference Comparison and Euclidean Distance	58
4.3.2	Statistical Analysis	59
4.3.3	3D Mapping Graph	61
4.3.4	Pearson Correlation Coefficient	62
4.4	Results Discussion	63
4.5	Sustainability and Environmental Friendly	65
4.5.1	SDG 3: Good Health and Well-being	65
4.5.2	SDG 9: Industry, Innovation, and Infrastructure	65
4.5.3	SDG 10: Reduced Inequalities	65
4.5.4	SDG 17: Partnerships for the Goals	65
CHAPTER 5 CONCLUSION AND FUTURE WORKS		67
5.1	Conclusion	67
5.2	Future Works	68

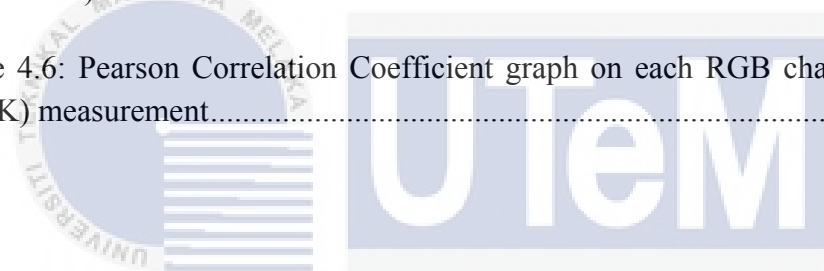
5.2.1	Exploration of Advanced Color Sensors for Enhanced Precision	68
5.2.2	Real Patient Analysis	69
5.2.3	Integration of Machine Learning Algorithms	69
5.2.4	Addition of Camera Module and Notification System	70
REFERENCES		72



LIST OF FIGURES

Figure 2.1: The Apgar score system [21].....	11
Figure 2.2: The dataset of Caucasian newborns' lip color presented in CIE 1976 L * a * b color space simulated by the developed color correction system from cyanosis to non-cyanosis color [24].....	13
Figure 3.1: The flowchart of the project	24
Figure 3.2: The 3D model design of the prototype's casing.....	25
Figure 3.3: The top view of the 3D model design	26
Figure 3.4: The side view of the 3D model design.....	27
Figure 3.5: The fabricated prototype's casing using 3D printing method	28
Figure 3.6: The front view of the fabricated prototype's casing.....	28
Figure 3.7: The schematic circuit of the CyanoMeter system	30
Figure 3.8: The circuit of the CyanoMeter system	30
Figure 3.9: RAL K7 color card which is used as skin color representation	33
Figure 3.10: RAL 8023 which represents the skin color	34
Figure 3.11: X-rite ColorChecker which is used for TCS34725 calibration	35
Figure 3.12: The illustration of measurement setup for LED (4150K) direct measurement	37
Figure 3.13: The direct measurement setup for LED (4150K).....	37
Figure 3.14: The illustration of measurement setup for bulb 3000K and 6500K	39

Figure 3.15: The measurement setup for bulb 3000K and 6500K.....	40
Figure 3.16: The Blynk's user interface for Cyanosis Detector	41
Figure 4.1: 3D scatter plot graph between theoretical and measured RGB values for LED (4150K) direct measurements	51
Figure 4.2: Pearson Correlation Coefficient graph on each RGB channels for LED (4150K) direct measurements	52
Figure 4.3: 3D scatter plot graph between theoretical and measured RGB values for bulb (3000K) measurements	56
Figure 4.4: Pearson Correlation Coefficient graph on each RGB channels for bulb (3000K) measurement.....	57
Figure 4.5: 3D scatter plot graph between theoretical and measured RGB values for bulb (6500K) measurements	61
Figure 4.6: Pearson Correlation Coefficient graph on each RGB channels for bulb (6500K) measurement.....	62



اونيورسيتي تيكنيكل مليسيا ملاك

UNIVERSITI TEKNIKAL MALAYSIA MELAKA

LIST OF TABLES

Table 2.1: Data lips from the first baby (Baby 1), going from cyanosis to non-cyanosis [24].....	13
Table 2.2: The comparison of specification and method for colorimeter	17
Table 3.1: The conversion of Dataset Lip 1 from CIEL * a * b to RGB [24]	31
Table 3.2: The conversion of Dataset Lip 2 from CIEL * a * b to RGB [24]	31
Table 3.3: The comparison of Dataset Lip 1 between actual and RAL K7 RGB values	32
Table 3.4: The comparison of Dataset Lip 2 between actual and RAL K7 RGB values	33
Table 3.5: Cyanosis and non-cyanosis status.....	42
Table 4.1: RAL K7 color reference comparison between theoretical and measured with Euclidean distance for LED (4150K) direct measurements.....	47
Table 4.2: Statistical analysis for LED (4150K)	48
Table 4.3: RAL K7 color reference comparison between theoretical and measured with Euclidean distance for bulb (3000K) measurements	53
Table 4.4: Statistical analysis for bulb (3000K) measurements	54
Table 4.5: RAL K7 color reference comparison between theoretical and measured with Euclidean distance for bulb (6500K) measurement.....	58
Table 4.6: Statistical analysis for bulb (6500K) measurements	59

LIST OF SYMBOLS AND ABBREVIATIONS

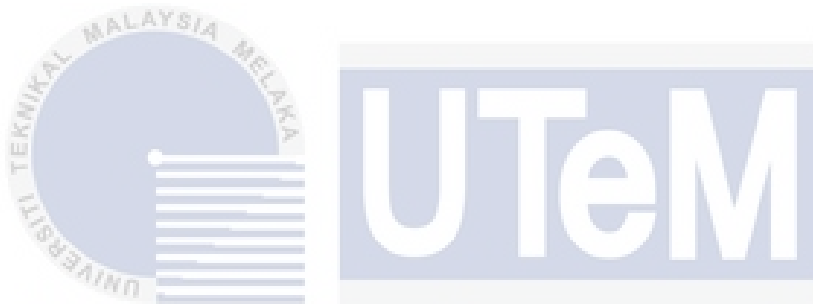
RGB : Red, Green, Blue

RAL : Reichs-Ausschuß für Lieferbedingungen und Gütesicherung



CHAPTER 1

INTRODUCTION



1.1 Background

Cyanosis is a common clinical finding in newborn infants, characterized by a bluish discoloration of the skin and mucous membranes due to an increased concentration of deoxygenated hemoglobin. This condition can be associated with significant and potentially life-threatening diseases, including pulmonary, cardiac, metabolic, neurologic, infectious, and hematologic disorders. The prevalence of respiratory distress in newborns, which can lead to cyanosis, ranges from 2.9% to 7.6% [1].

The most common cause of central cyanosis in newborns is respiratory distress, including conditions such as hyaline membrane disease, transient tachypnea of the newborn, meconium aspiration, and pneumonia [2]. Cyanosis resulting from the right-to-left shunt typically presents in adolescence or adulthood [3]. In addition to respiratory causes, pulmonary disorders such as primary lung disease, airway

obstruction, and extrinsic compression of the lungs can also lead to cyanosis in newborns [4]. Methemoglobinemia, although rare, is another potential cause of cyanosis in newborns [5]. For proper diagnosis and management, it is important to differentiate between cardiovascular and pulmonary causes of cyanosis in newborns [4]. Cyanosis in newborns is characterized by a bluish discoloration of the skin, mucus membranes, and nail beds [6]. In a recent series of newborn dermatoses, acrocyanosis was noted in approximately 12% of infants, with no variation based on skin color [7]. In the absence of central cyanosis or evidence of systemic illness with anemia, polycythemia, jaundice, or respiratory distress, acrocyanosis is considered a benign finding that resolves within days.

The traditional methods for detecting cyanosis in newborns include complete blood count, pulse oximetry, and hyperoxia test [8]. However, these methods require direct contact with the infant and may not be efficient for continuous monitoring. Therefore, there is a need for a non-invasive, efficient, and reliable method for detecting cyanosis in newborns.

1.2 Problem Statement

Newborns can suffer from cyanosis, a medical condition that can lead to severe health complications if not detected and treated promptly. One non-invasive method for detecting cyanosis is transcutaneous oximetry, which measures oxygen saturation in the blood that have limitations in availability, reliability, and continuous monitoring [9]. These gaps necessitate developing a new approach for cyanosis detection that is accurate, affordable, and user-friendly. Training medical professionals to identify cyanosis through visual skin color assessment is essential but lacks an objective quantification method. Previous training relies on subjective color analysis which can be inconsistent. There is a clear need for an easy-to-use and reliable device to detect,

quantify, and monitor cyanosis levels to aid medical training. Thus, it is essential to train new medical professionals in quantifying and identifying cyanosis coloration in newborns, and this device will make such training easier by providing a simple way for trainees to practice measuring cyanosis levels and correlating color values with cyanosis severity. An IoT-based device using the TCS34725 color sensor can be a potential solution to this problem. The device will be designed to measure bluish discoloration on newborn skin, particularly around the lips, to determine cyanosis level. The device will integrate an ESP32 microcontroller for data processing and transmission, a color sensor, an LCD screen, and a push button for user interface. This affordable device aims to improve training by enabling objective quantification of cyanosis levels from color data.

1.3 Objectives

The primary objective of this study is to develop and evaluate an IoT-based cyanosis detection device using the TCS34725 color sensor for newborn assessment in medical training applications. Specific objectives include:

- i. To develop a non-invasive device to detect cyanosis by using color sensor to measure the color values in RGB space.
- ii. To analyze the color values via an IoT implementation.

1.4 Significance of the Study

The research's importance lies in its numerous contributions to medical diagnostics. First, it enables better diagnosis by providing a reliable way to detect cyanosis in newborns. The non-invasive approach is also significant as it ensures a gentle detection process that does not require direct contact with the infant. Additionally, the

study introduces remote monitoring and analysis, which allows healthcare professionals to assess a newborn's condition from afar, promoting efficient healthcare management. The cost-effective nature of the proposed solution adds another layer of significance by making it accessible and feasible for healthcare settings with varying resource levels. Furthermore, the study offers promise for early intervention by enabling healthcare providers to promptly identify cyanosis and take necessary actions, potentially leading to improved outcomes for affected infants. Beyond its technical aspects, this study has practical applications that can positively impact neonatal healthcare.

1.5 Scope of the Study

The study encompasses the complete development of the Transcutaneous CyanoMeter device, involving various crucial phases. Initially, it involves designing and engineering the device meticulously to ensure functionality and effectiveness. The selection and integration of advanced color sensor technology are essential, prioritizing precision and reliability in color measurements.

The study also covers the development of the measurement device while considering factors such as usability, non-invasiveness, and practicality in healthcare settings. Calibration and validation processes ensure that the CyanoMeter provides accurate and consistent color readings, particularly when detecting cyanosis in newborns.

Apart from device development, the scope includes an innovative IoT implementation which integrates IoT techniques for remote analysis and processing of color values obtained by the device. This aspect extends its utility by enabling real-time monitoring and analysis for more efficient neonatal healthcare practices.

This study's scope is extensive as it covers all stages of developing transcutaneous CyanoMeter, from conceptualization through design to implementing IoT for enhanced functionality with remote capabilities.

1.6 Organization of the Thesis

The thesis comprises individual sections, each offering a distinct contribution to the study of identifying cyanosis in newborns and utilizing Internet of Things devices in healthcare. In Chapter 2, an extensive examination of existing literature on these subjects is presented, encompassing various perspectives on detecting cyanosis in newborns.

In Chapter 3, there is a comprehensive elucidation of the intricate process involved in creating a new device for detecting cyanosis. This section delves into both the technical aspects of the gadget and provides insights into the considerations, methodologies, and decision-making processes that influenced its development - covering everything from conceptualization to practical implementation.

Chapter 4 marks the culmination of empirical exploration within this thesis by presenting thorough validation tests' results. This chapter offers an exhaustive review of research findings with each outcome carefully evaluated for its significance in infant care and medical training. The detailed analysis establishes a link between theoretical and practical aspects by connecting the developed device's functionality with its potential real-world effects.

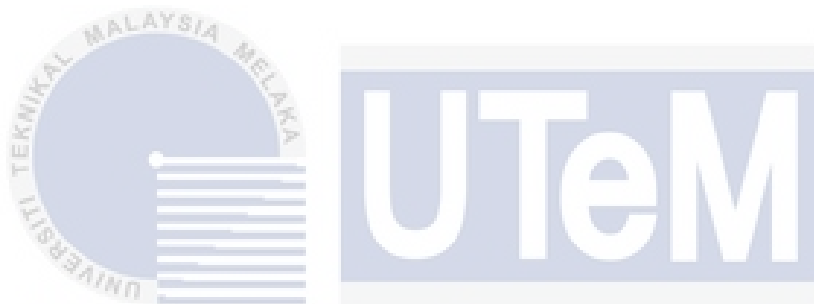
Finally, Chapter 5 encapsulates synthesis and conclusion where it summarizes key research findings while suggesting avenues for future studies. Alongside reflecting on

past accomplishments, this section proposes new areas for exploration aiming at innovative progress concerning newborn healthcare as well as IoT applications.



CHAPTER 2

BACKGROUND STUDY



Background studies are necessary to achieve the goals of the project and to ensure that it is based on sound scientific principles. Several studies related to colorimetry and medical diagnosis of cyanosis will be considered to develop the project.

2.1 Cyanosis

Cyanosis is a clinical sign that is characterized by a bluish discoloration of the skin, mucous membranes, and nails due to the presence of deoxygenated hemoglobin in the blood [10]. It is a common manifestation of various medical conditions, including congenital heart disease, chronic obstructive pulmonary disease, and acute myocardial infarction. The severity of cyanosis is determined by the amount of reduced hemoglobin in the capillaries, which is necessary to cause cyanosis [11].

The first paper by Ling Y., Li T., and An Q. discusses on a 1-year-old infant presented to the emergency department for cyanosis, which happened suddenly after crying and screaming, mainly concentrated around the lips, and lasted for approximately 2 hours as mentioned in this paper [12]. The baby displayed sudden blueness around the mouth after crying, along with challenges in feeding, spitting up milk, and an increase in bowel movements.

The second paper by Shin C., Hong M., and Kim M. et al. discusses on case report of a newborn with cyanosis and Hb M Boston mutation [13]. Low levels of oxygen in pulse oximetry readings, even when arterial blood saturation is normal, may indicate Hb M disease in newborns presenting with cyanosis or low SO₂ on pulse oximetry. This holds true regardless of MetHb value.

The third study conducted by Laskine-Holland M., Kahr W., Crawford-Lean L. et al. found that cyanotic children showed reduced clot firmness in the fibrinogen/fibrin polymerization aspect of the clot when compared to noncyanotic children [14]. However, differences in hematocrit, platelet count, and sex between groups accounted for the association between cyanosis and clot firmness. The study suggested that cyanosis could impact coagulation in children with congenital heart defects.

The fourth paper by Cordina R., Grieve S., Barnett M. et al. examines the impact of persistent cyanosis in adults with congenital heart disease, exploring alterations in brain structure and neurological function among this group [15]. The findings indicate that individuals with cyanosis demonstrate widespread indications of diminished brain volume, alongside particular areas where cortical thickness is reduced. These observations suggest that factors such as inflammation, neurohormonal activation, and

endothelial dysfunction may play significant roles in the development of these changes.

The fifth paper by McNamara R., Taylor C., McKenzie D. et al. Elaborates on the challenges of identifying cyanosis, a condition marked by a bluish tint of the skin, in people with color vision deficiencies [16]. This study confirms that the alteration in color linked to cyanosis poses a difficulty for observers with color vision deficiencies. The findings indicate the nature of this color change and validate previous informal observations about the problems experienced by individuals with CVDs when detecting cyanosis.

2.2 Apgar Score

The Apgar Score is a brief and standardized tool used to assess the immediate physical condition of a newborn baby after birth. Named after its creator, Dr. Virginia Apgar, this scoring system assigns numerical values to five main criteria: Appearance, Pulse, Grimace response, Activity, and Respiration. The assessment is typically conducted at one and five minutes post-delivery to provide a quick overview of the infant's overall well-being. It assists medical professionals in making timely decisions regarding any necessary interventions or additional care for the newborn. Despite its simplicity, the Apgar Score has proven to be an important and widely accepted tool in evaluating newborns' health status shortly after delivery. Cyanosis, which is characterized by a bluish discoloration of the skin, is one of the criteria assessed in the Apgar Score and can indicate potential issues with the baby's respiratory system.

Ahmed M. and Kamel I.'s paper explores the Apgar scoring system, which is employed to evaluate the well-being of newly born infants [17]. This method evaluates color, heart rate, reflexes, muscle tone, and respiratory effort with a range of 8 to 10

indicating normalcy. The Apgar scoring system serves as a widely recognized tool for neonatal assessment where a score between 0 and 3 signifies fetal distress necessitating urgent resuscitation.

The second study conducted by Lin L., Liu G., and Li Y. et al. examines the link between Apgar scores and the likelihood of survival among extremely preterm infants born at 25-27 weeks gestation [18]. The research describes the distribution of Apgar scores in these infants and investigates how Apgar score is associated with survival rate at discharge using clinical data from extremely preterm infants discharged from 26 neonatal intensive care units in Guangdong Province, China between January 2008 and December 2017.

Te Pas A. and Witlox R.'s third paper discusses the questioning of the reliability and validity of the Apgar score [19]. Despite being utilized for over 50 years to predict newborn outcomes at birth, as outlined by the authors, it has been widely acknowledged as a trustworthy and accurate measure.

Rozycki H. and Yitayew M.'s fourth paper examined the utilization of the Apgar score in clinical research publications, as well as its users and potential changes in usage patterns from 1989-90 to 2018-19 [20]. The study revealed that the primary application of the Apgar score was for evaluating newborn status following pregnancy/delivery interventions. Furthermore, there is a lack of uniform definition for what constitutes a significant Apgar score.

Blake D.'s fifth paper proposes a reassessment of the Apgar score's 'color' component and advocates for the implementation of a revised system to effectively evaluate the healthy newborn's color post-delivery [21]. The current application of the

'color' observation within the Apgar score is deemed inappropriate in relation to the physiological transitions from fetal to neonatal life, thus warranting a comprehensive review.

Sign/observation	Score 0	Score 1	Score 2 points
Activity (muscle tone)	Absent	Some flexion	Active movement
Heart rate	Absent	Below 100 beats per minute	Above 100 beats per minute
Grimace (reflex irritability response to stimulation)	No response to stimulation	Grimace/feeble cry	Sneeze, cough, pulls away
Appearance (skin colour)	Blue all over (or white)	Centrally pink with blue extremities	Pink all over
Respiration/breathing	Absent	Slow, irregular, weak	Regular, crying

Figure 2.1: The Apgar score system [21]

Many research papers have consistently raised issues about the reliability of the Apgar scoring system, urging for its modification. The main problem identified is the subjective nature of the assessment process, which causes differences in scores between different assessors. Relying on subjective judgments presents a major challenge, leading researchers to highlight the importance of an objective and standardized approach to improve accuracy and consistency in evaluating newborns' immediate health status using the Apgar scoring system.

2.3 RGB Color Space

The RGB color model, commonly used in digital devices and light-based media, is based on adding different intensities of red, green, and blue to create a wide range of colors. Each color channel in the RGB model is represented by an intensity value from 0 to 255. When all channels are at maximum intensity, white is produced; conversely, when there is no intensity in any channel, black is created. The additive nature of the RGB model allows for the combination of primary colors' wavelengths and makes it well-suited for computer screens and web applications. Its versatility lies in its

capability to generate numerous colors by making simple adjustments to the three color channels.

It has diverse statistical graphics, data visualizations, and image processing applications. The color space package in R offers tools for selecting individual colors or color palettes based on the HCL color space, which closely aligns with the human visual system and facilitates intuitive color palette selection [22]. Additionally, methods and devices exist for compressing the RGB color space to reduce chromatic aberration and enhance algorithm effectiveness. Moreover, a new technique utilizing overlapping RGB LEDs has been proposed to improve system reliability and capacity in optical camera communication through an enhanced 2-D diversity approach within the RGB color space [23]. Overall, the RGB color model is fundamental in representing colors with various practical applications across different fields.

2.4 Cyanosis Color Values

The study by Azmi N., Delbressine F., and Feijs L. et al focuses on image-processing strategy to identify cyanosis in infants [24]. The procedure entails the identification of the cyanosis region of interest in the images, followed by using an algorithm to adjust the color and calibrate the images. Subsequently, a database of cyanosis CIE $L^*a^*b^*$ (CIELAB) values is generated. The study employed an uncalibrated Sony Cyber-shot DSC-RX 100 type III camera to photograph infants exhibiting cyanosis. The findings demonstrated that the suggested approach successfully identified cyanosis in newborns with a precision rate of 95.5% [24].

Additionally, the study proposes that the suggested system might be employed during training sessions for medical practitioners to evaluate babies more impartially. The discussion emphasizes the significance of precisely evaluating cyanosis in

neonates to detect and treat pulmonary disease and congenital cardiac conditions effectively. The study also recommends that future research incorporate a more significant number of photos depicting neonates exhibiting diverse cyanosis discoloration and infants with a range of different skin color types.

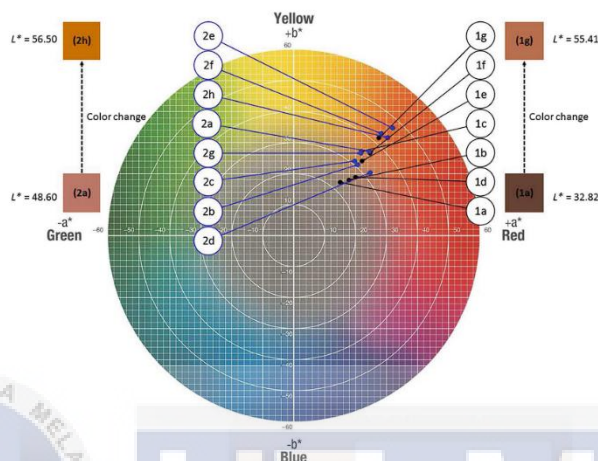


Figure 2.2: The dataset of Caucasian newborns' lip color presented in CIE 1976 L * a * b color space simulated by the developed color correction system from cyanosis to non-cyanosis color [24]

Table 2.1: Data lips from the first baby (Baby 1), going from cyanosis to non-cyanosis [24]

	*L	*a	*b
1	32.8	14.78	15.18
2	41.71	18.84	18.64
3	39.1	22.35	25.49
4	50.45	20.95	19.91
5	49.1	22.48	24.29
6	51.53	24.66	27.21
7	55.41	28.52	31.05

2.5 Harnessing Color Vision

Central cyanosis is characterized by a bluish tint of the skin, lips, tongue, nails, and mucous membranes and is caused by inadequate oxygenation of the arteries. It has long been recognized that oxygen saturation is at a dangerously low level when skin color indicators become apparent. The challenge in identifying core cyanosis mainly stems from the limited ability of our eyes to perceive subtle changes in skin color. Core cyanosis exhibits little spatial color gradients, which makes it challenging for viewers to notice. The "skin-tone adaptation" technique is based on the well-established principle that our ability to perceive color differences is enhanced when the backdrop color closely resembles the colors being compared [25].

Consequently, it is advisable for bedding, gowns, walls, and other objects close to a patient to be of a skin-toned color, ideally closely like the patient's skin tone. By doing this, it enhances the ability of a viewer with normal color vision to perceive subtle changes in skin color. The concept proposes replacing the current white walls and linens in hospital and clinic rooms, as well as the commonly blue or green patient gowns, with colors that match the natural tone of human skin. "Biosensor color tabs" refer to adhesive tabs that a clinician strategically inserts on the patient's skin at various locations [25]. The practitioner can select tabs from an extensive range of flesh-toned hues, enabling them to identify a suitable match for the patient's skin tone. The tabs function as biosensors that can detect changes in perception. Similar to how a clinician may use a marker to mark a rash and track its size over time, placing a tab that matches the patient's skin tone on their skin allows the observer to monitor any changes in skin coloration at a later point. For instance, if the skin constantly shifts towards the blue spectrum, a previously colorless and barely noticeable skin tab, initially matched to the previous skin color, will abruptly become vivid and yellow. As the skin color

change increases, the perceived saturation of the tab becomes stronger. With the presence of these biosensors, central cyanosis can be detected at far greater levels of oxygen saturation, ensuring safety.

2.6 Colorimeter in detecting colors

A color sensor is a device designed to measure the color of objects and the intensity of light that reaches the sensor. It operates by utilizing light for identifying and examining various colors, responding to diverse colored solutions through different spectral bands for each sensor channel [26]. This technology allows for quantitative optical analysis of colored solutions and can identify electromagnetic radiation reflected by samples, offering a linear range for dye solutions suitable for colorimetric substance determination [27]. Customization of the sensor's characteristics can be achieved using both sensor elements and color filter elements, while application in a dedicated module facilitates precise recognition of object colors while minimizing interference from ambient light sources.

The study by Beyaz A. discusses the efficacy of low-cost colorimeters based on Arduino technology in assessing various agricultural products [28]. The authors employed four distinct cost-effective color sensors (TCS3200, TCS34725, APDS-9960, and VEML6040) in conjunction with an Arduino microcontroller to quantify the color properties of various agricultural commodities (apple, tomato, lemon, and banana). In addition, a spectrometer was employed as a benchmark instrument to assess the accuracy and precision of the color sensors. The researchers utilized linear regression and calibration approaches to enhance the efficacy of the color sensors. According to the authors, the TCS34725 sensor demonstrated superior accuracy and precision compared to the other three-color sensors, with the TCS3200 sensor coming

in second [28]. The accuracy and precision of the APDS-9960 and VEMML6040 sensors could have been improved, particularly in the blue and green channels. The researchers also discovered that the calibration parameters exhibited variations based on the specific agricultural commodity and the color channel utilized. The researchers determined that the Arduino-based color sensors may be a cost-effective substitute for the pricey spectrometer in some agricultural applications. However, additional enhancements and validation were necessary.

The study carried out by de Carvalho G., Machado C., Inácio D et al. investigates the utilization of an RGB color sensor for accurate optical examination of colored solutions [27]. The paper examines the use of a red, green, and blue color sensor to quantitatively analyze colored solutions and assesses its ability to detect various colors, aiming to gain insight into which spectral bands are filtered and processed by each sensor channel. The research includes an assessment of the response of the RGB color sensor to different colored solutions and a quantitative analysis method using the RGB sensor. It was found that the RGB color sensor has a range of 415-564 nm for blue, 440-600 nm for green, and 510-750 nm for red channels. Moreover, it exhibited a linear range from 5.0-50.0 $\mu\text{mol L}^{-1}$ for dye solutions [27].

The study by Siu V., Lu M., Hsieh K. et al. presents an inexpensive and portable device for accurately measuring nitrite in urine, which could aid in the early identification of urinary tract infections [29]. This innovative and affordable transmission-based colorimeter has potential for broadening its application to detect various biomarkers, thus enhancing the overall precision and accuracy of the intended analysis. The approaches utilized encompass traditional methods such as visual assessment of urinary dipsticks or using a reflectance spectrophotometer, alongside a

new technique involving a transmission-based colorimeter for quantifying nitrite levels. The findings indicate that this colorimeter exhibits greater sensitivity compared to commercial dipstick analyzers, facilitating earlier detection of urinary infections [29].

2.6.1 Summary of Colorimeter Specifications

Cyanosis in newborns, which can be a life-threatening condition, may result from various factors such as pulmonary disorders, airway obstruction, external compression of the lungs, and congenital heart defects. It is essential to assess and distinguish these causes carefully in clinical practice. Early detection and prompt treatment of cyanosis are crucial as they could indicate a serious underlying health issue in neonates. Having a reliable device for promptly detecting cyanosis is vital for newborn care. The device's specifications must be thoughtfully considered to ensure accurate and timely detection of cyanosis in newborns; this includes sensitivity, specificity, ease of use, and portability considerations.

Table 2.2: The comparison of specification and method for colorimeter

References	Color Sensor	Methods	Application
[29]	Photodetector	- a transmission-based colorimeter for quantitative measurement of nitrite.	Early detection of urinary tract infections (UTIs).
[27]	TCS34725	- Evaluation of the RGB color sensor's response to different colored solutions.	Colorimetric determination of iron in soil and

		<ul style="list-style-type: none"> - Quantitative analysis of colored solutions using the RGB sensor. 	<p>supplement samples.</p>
[28]	TCS3200, TCS34725, APDS-9960, and VEML6040	<ul style="list-style-type: none"> - Measurement on Granny smith apple, Starkrimson apple, and Plum using all color sensors. - 20 samples selected and 50 measurements have been managed for each target object. 	<p>Comparison of Arduino Based Inexpensive Colormeters Effectiveness at Some Agricultural Products</p>
[30]	TCS3200	<ul style="list-style-type: none"> - Construction of Colorimeter CK20.1 prototype using TCS3200 sensor and Arduino Mega-2560 microcontroller. - Validation of prototype quality performance using ColorFlex EZ Spectrophotometer. 	<p>Colorimeter design for dry food-products inspection</p>
[31]	Photodiode	<ul style="list-style-type: none"> - Putting the sample between RGB and photodiode. 	<p>Colorimetry system for food dye determination</p>

[32]	TCS3200	<ul style="list-style-type: none"> - Synthesis of azophenol-based chromogenic probe for colorimetric analysis - Development of a colorimetric device using a color sensor and Arduino microcontroller 	‘Color to concentration’ quantification of cyanide in real samples
[33]	TCS3200	<ul style="list-style-type: none"> - Integration of four photodiode arrays on the metasurface for active sensing on trichromatic colors and real-time response in scattering field control. - Design of a 1-bit programmable unit using FPGA hardware system to regulate the reflected phase response of scattering fields. 	Trichromatic-color-sensing metasurface with reprogrammable electromagnetic function
[34]	TCS3200	<ul style="list-style-type: none"> - Gas sensor (TGS 2602) and color sensor (TCS 3200) are used. 	Honey Quality Tool

		- The microcontroller used is NodeMCU ESP32.	
[35]	TCS34725	- Using a controller with color temperature feedback from a sensor enables the creation of various modes and light scenes.	Measurement of Correlated Color Temperature
[36]	TCS3200	- Color sensor measuring the bilirubin level. - The device consists of an RGB color sensor, microcontroller, and LCD display.	Bilirubin jaundice (BiliDice) device for neonates

In conclusion, early detection of cyanosis in newborns is a crucial aspect of healthcare intervention due to its link with potentially life-threatening conditions such as pulmonary disorders, airway obstruction, and congenital heart defects. The research presented has examined various color sensors and techniques, offering valuable insights into their uses, effectiveness, and potential in neonatal care.

The reviewed color sensors - TCS34725, TCS3200, APDS-9960, VEML6040, and photodiodes - have been utilized in diverse applications from urinary tract infection detection to determining iron levels in the soil by colorimetry. These studies have also explored the application of color sensors for food quality inspection, gas sensing, and even measuring bilirubin levels in neonates.

Significantly, the research underscores the importance of developing a reliable device for prompt and accurate cyanosis detection in newborns. Critical considerations for such a device include sensitivity, specificity, ease of accessible usage, and portability. The referenced studies add to the broader understanding of color sensor applications which can pave the way for innovative devices like CyanoMeter for improved neonatal healthcare.

The wide range of showcased applications emphasizes the flexibility of color sensors, supporting their integration into medical devices for varied diagnostic purposes. As technology progresses, these findings highlight potential future innovations, particularly affecting advances in healthcare represented within neonatal care.

Within the context relating to affiliated with the CyanoMeter project, the literature review enables comparisons with existing designs, providing base knowledge aiding further refinement and leaving room for more advanced research, which will drive forward development plans.

Insights gained from these investigations contribute towards creating a dependable tool that will positively impact the enhancement of neonatal medical care through comprehensive preliminary assessment activities. Overall, the literature review highlights the significance of accurate and efficient cyanosis detection in newborns for timely medical intervention.

2.7 Summary of the literature review

Research evaluating cyanosis in newborns has revealed significant gaps in this condition's objective quantification and monitoring. The visual assessment of cyanosis

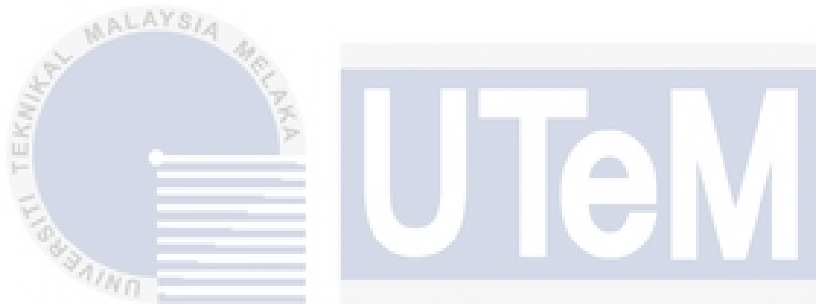
is subjective and lacks consistency, while pulse oximetry has limitations in detecting mild cyanosis [19], [21]. Additionally, the Apgar score's 'color' grading is considered unreliable for assessing cyanosis severity. Prior studies have explored extracting cyanosis color features from images, but a real-time quantification device remains to be developed.

While principles of color perception show promise for improving cyanosis detection, practical tools based on this concept require further exploration [25]. Although color sensors have been used for medical applications, their potential for monitoring cyanosis has not yet been thoroughly investigated [12]. These identified knowledge gaps motivate the current study to address these deficiencies by developing an easy-to-use IoT-based device utilizing the TCS34725 color sensor to quantify cyanosis through colorimetry.

Establishing a link between background information and the problem statement reveals that existing methods for detecting cyanosis are unreliable according to literature review findings; therefore, there is a need to develop an objective methodology through this study. Addressing the lack of real-time tools based on color analysis with a proposed device utilizing new technology provides strong justification for the conduction of this research.

CHAPTER 3

METHODOLOGY



This chapter includes every aspect of the methodological project, including a flow chart, prototype design, mathematical calculations, and thorough project descriptions.

This chapter provides a smooth implementation of the project's planning and a thorough explanation of the project's comprehension.

3.1 Flowchart

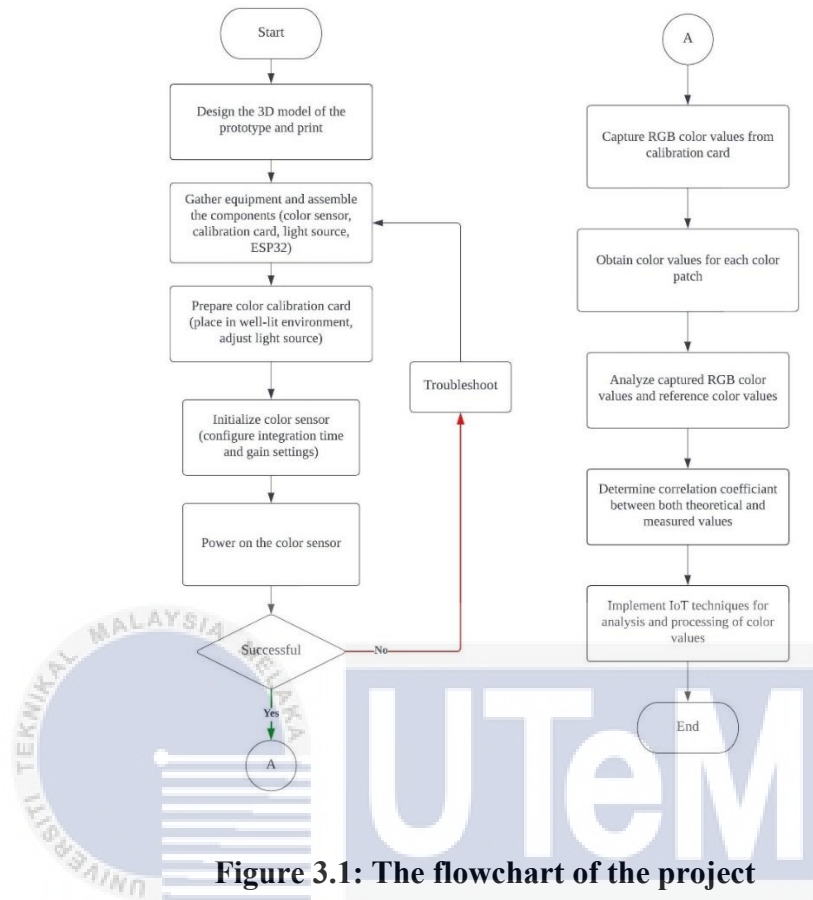


Figure 3.1: The flowchart of the project

The CyanoMeter is a device specifically designed to identify central cyanosis in infants. The development process of the CyanoMeter adheres to a methodical procedure, commencing with the creation of a 3D model and the precise 3D printing of the prototype. The essential elements, including the color sensor, calibration card, light source, and ESP32 microcontroller, are intentionally integrated to attain the best possible performance.

After completing the prototype, the focus shifts to preparing the color calibration card in a brightly illuminated setting. Accurate calibration of the light source is crucial to guarantee precise color measurements, which is vital in maintaining the CyanoMeter's precision. The color sensor is configured and initialized, with meticulous adjustment of integration time and gain properties. The

RGB color values are obtained from the calibration card, which serves as a fundamental dataset for analysis. Evaluating the CyanoMeter's performance involves comparing the individual RGB readings and the expected values to accurately determine its ability to depict color.

The features of the CyanoMeter are enhanced in the final stage by integrating Internet of Things (IoT) technology, thereby improving its data processing, analysis, sharing, and storage abilities. The device's strategic integration ensures it meets the criteria for reliably and efficiently managing color data to detect central cyanosis in infants, and efficiently managing color data to identify central cyanosis in babies.

3.2 Prototype Design and Fabrication

3.2.1 3D Model Design

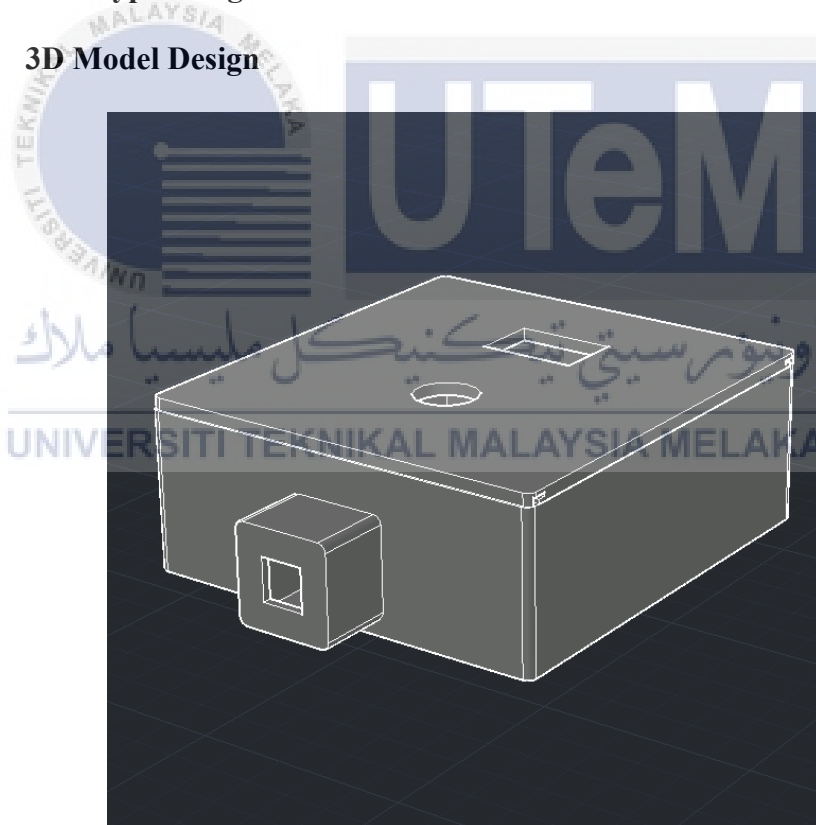


Figure 3.2: The 3D model design of the prototype's casing

The innovative design of the CyanoMeter prioritizes both safety and ease of use. Its compact dimensions (110x100x40) and rounded corners effectively protect babies while emphasizing user safety. The detachable top, known as the "cover", is

constructed with a sliding mechanism and strategically placed hinges to prevent accidental separation, enhancing security and convenience.

The sliding mechanism lets users easily access internal components by moving the lid. This user-friendly approach ensures reliable measurements during operation, boosting the prototype's reliability. The CyanoMeter is committed to achieving excellence in aesthetics and practicality through its carefully designed features, such as rounded edges for safety and a sliding lid mechanism for user comfort.

With meticulous attention to detail in incorporating features like rounded edges for safety and an easy-to-use sliding lid mechanism, this well-crafted design reflects a dedication to excellence in aesthetics and functionality. It exemplifies the ingenuity of its design process and development precision. The CyanoMeter's design is a testament to the careful consideration of safety and user-friendliness.

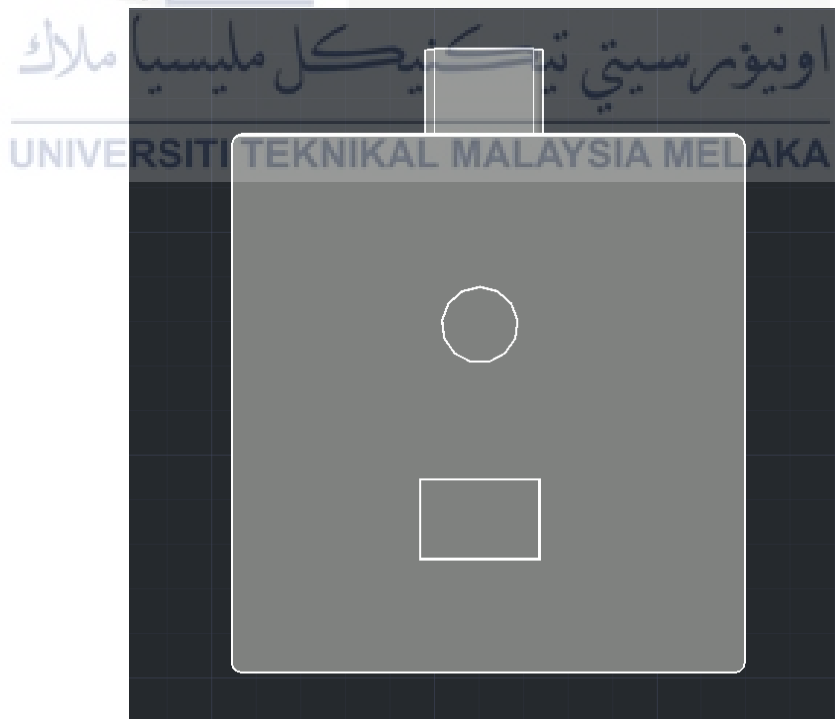


Figure 3.3: The top view of the 3D model design

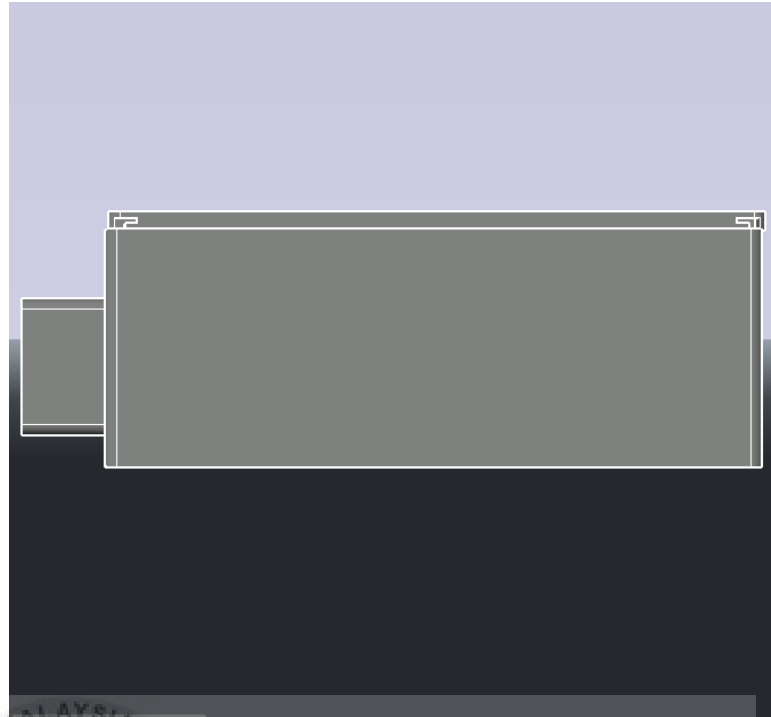


Figure 3.4: The side view of the 3D model design

3.2.2 Fabrication

Creating a physical representation from a virtual design involved using advanced 3D printing technology. This process ensured that the intricate details of the CyanoMeter model were accurately reproduced with great precision. The deliberate focus on user safety was evident in the design, which included rounded edges to minimize any potential risk of infant injury and incorporated child-proof features. The fabrication stage brought the concept into reality and highlighted the meticulous planning and attention to detail invested in producing the CyanoMeter, ensuring it met high safety standards for its intended users.



Figure 3.5: The fabricated prototype's casing using 3D printing method



Figure 3.6: The front view of the fabricated prototype's casing

3.3 Circuit Components

The ESP32 microcontroller board manages all the processing requirements of the circuit. The ESP32 controls the overall operation of the CyanoMeter and facilitates seamless integration with IoT through WiFi connectivity. Consequently, the equipment can transmit and receive data, enhancing its efficiency and enabling remote control and monitoring.

The Input Button is represented by a red switch featuring a push button. It serves as the interface component for initiating color measurements. The CyanoMeter offers a user-friendly input mechanism that ensures easy interaction and promotes user engagement.

The Display Module, a compact OLED screen, is crucial for visually presenting the results of color measurements. When connected to the microcontroller, this component retrieves data from the color sensor, analyses it, and displays the results. The OLED display's real-time visual representation enables a user-friendly experience by providing consumers instant feedback.

The color sensor module, a vital circuit part, contains the TCS34725 color sensor, which accurately measures color values. When connected to the microcontroller, this sensor captures data regarding the color of the sample.

The CyanoMeter relies on a 9V power supply as its primary power source, ensuring the circuit operates efficiently by delivering the required voltage. This power input guarantees sufficient power to enable smooth operation, supporting the different components such as the ESP32 microcontroller, Input Button, Display Module, and Sensor Module.

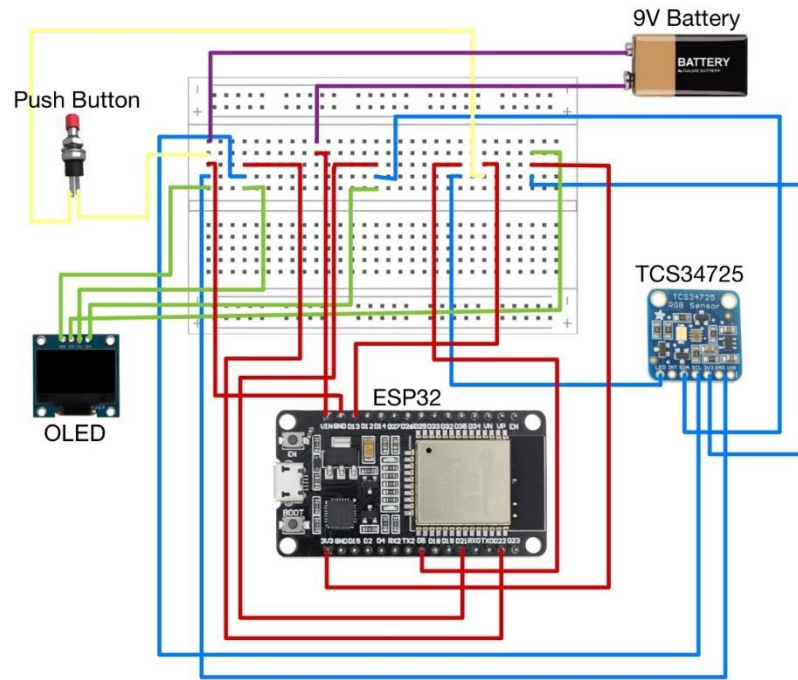


Figure 3.7: The schematic circuit of the CyanoMeter system

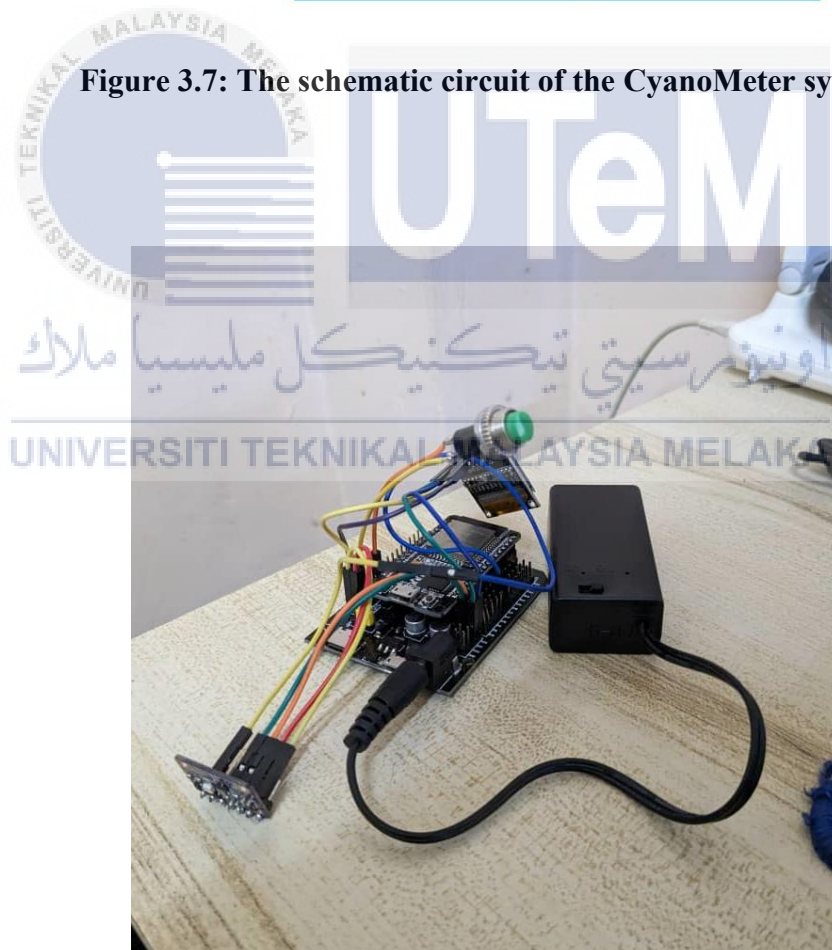


Figure 3.8: The circuit of the CyanoMeter system

3.4 Color Reference Selection

3.4.1 Dataset Lip Selection

The dataset containing color references for babies with cyanosis and without cyanosis was acquired from the research paper by Azmi N., Delbressine F., Feijs L. et al. [24]. The dataset was initially in the CIEL * a * b color space, which is a color space that provides a uniform perception of colors. To match the RGB color readings of the CyanoMeter, a conversion from CIEL * a * b to RGB was carried out using a free online color converter tool to convert between CIEL * a * b and RGB color spaces [37]. The tool facilitated effortless conversion between many color systems such as CIEL * a * b, HEX, sRGB, CMYK, and XYZ. The RGB values acquired from this conversion were the basis for later color analysis.

Table 3.1: The conversion of Dataset Lip 1 from CIEL * a * b to RGB [24]

Dataset Lip 1			Actual		
*L	*a	*b	R	G	B
32.82	14.78	15.18	104	68	54
41.71	18.84	18.64	134	86	89
39.1	22.35	25.49	133	77	52
50.45	20.95	19.91	161	106	87
49.1	22.48	24.29	160	101	77
51.53	24.66	27.21	171	106	78
55.41	28.52	31.05	188	112	80

Table 3.2: The conversion of Dataset Lip 2 from CIEL * a * b to RGB [24]

Dataset Lip 2			Actual		
*L	*a	*b	R	G	B

48.6	24.79	27.34	163	98	70
44.85	20.2	23.07	145	93	69
43.18	20.34	24.79	141	88	62
57.63	25.87	20.64	188	120	104
59.36	32.97	35.03	207	118	83
57.62	28.19	33.13	194	118	82
47.44	22.98	27.69	157	97	67
56.5	30.54	32.95	194	113	80

3.4.2 RAL K7 Comparison

The converted RGB values of the dataset's lips were compared to the RAL K7 color fan to generate a dependable depiction of skin color. The RAL K7 is widely recognized for its extensive range of skin color patches, making it an excellent resource for studying differences in skin tone. Every color patch in the RAL K7 contains RGB values as theoretical references. By analyzing the dataset's lip RGB values and comparing them to the RAL K7, we could determine the color code that most closely matched the lip colors of the babies. This rigorous method guaranteed the selection of precise skin color representations for later assessments.

Table 3.3: The comparison of Dataset Lip 1 between actual and RAL K7 RGB values

Dataset Lip 1	Actual			RAL K7		
	R	G	B	R	G	B
RAL 8007	104	68	54	112	69	42
RAL 8025	134	86	89	117	88	71
RAL 8004	133	77	52	141	73	49
RAL 1011	161	106	87	175	128	79
RAL 8000	160	101	77	137	105	62
RAL 1011	171	106	78	175	128	79
RAL 3022	188	112	80	207	105	85

Table 3.4: The comparison of Dataset Lip 2 between actual and RAL K7 RGB values

Dataset Lip 2	Actual			RAL K7		
	R	G	B	R	G	B
RAL 8023	163	98	70	164	87	41
RAL 8024	145	93	69	121	80	56
RAL 8024	141	88	62	121	80	56
RAL 1024	188	120	104	186	143	76
RAL 3022	207	118	83	207	105	85
RAL 3012	194	118	82	198	132	109
RAL 3016	157	97	67	166	61	47
RAL 3012	194	113	80	198	132	109



Figure 3.9: RAL K7 color card which is used as skin color representation



Figure 3.10: RAL 8023 which represents the skin color

3.4.3 Practical Challenges in Lip Color Measurement

Accurately measuring the lip colors of infants is challenging due to practical impediments, such as motion and sensitivity. The RAL K7 color references were used as substitutes for lip colors to find a practical solution. The RAL K7 color palette has a wide array of red, pink, and brown shades that closely imitate the natural variations in lip color. By utilizing these color samples, it was possible to thoroughly represent various skin tones, enabling the accurate adjustment and verification of the sensor's performance.

3.5 Color Sensor Accuracy Experiment

3.5.1 TCS34725 Calibration

The X-Rite ColorChecker was an essential tool for the color sensor calibration process, providing a standardized reference. Its meticulous design and widespread acceptance of color calibration ensured reliable calibration results in the experimental setup. With its grid containing various well-defined and consistent color patches, the ColorChecker served as a benchmark for systematically comparing the color sensor's measurements against its known values. Leveraging these known color values, the calibration process aimed to improve the accuracy and reliability of color measurements across different hues, establishing a solid basis for subsequent analyses.

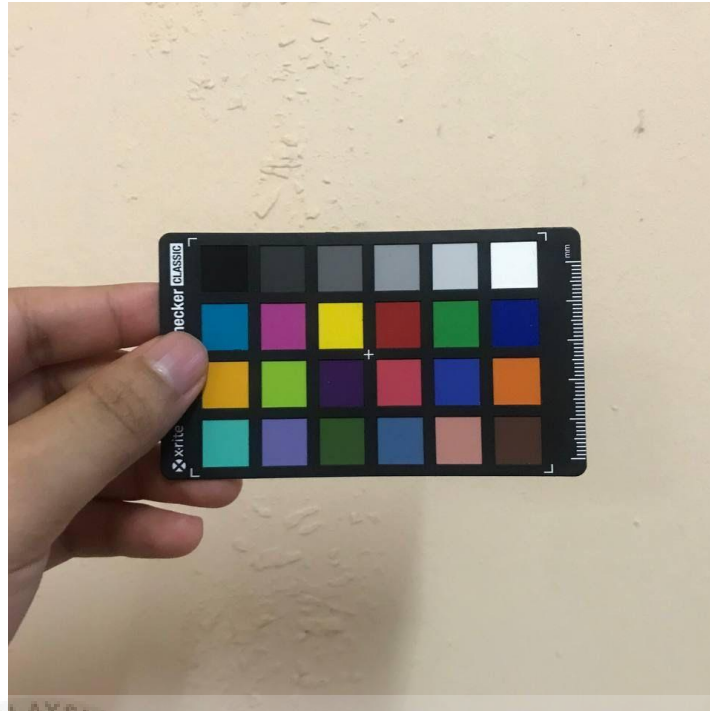


Figure 3.11: X-rite ColorChecker which is used for TCS34725 calibration

3.5.2 Experimental Lighting Sources

The color sensor accuracy experiment was carried out with great regard to detail and thoroughness, putting the CyanoMeter to assessment under three different lighting conditions. The decision to do this was to thoroughly assess the color sensor's effectiveness under various lighting conditions. The three chosen illumination sources comprised a 4150K LED, a 3000K bulb, and a 6500K bulb, each representing distinct color temperatures. The deliberate incorporation of several lighting circumstances offers a comprehensive and precise assessment of the CyanoMeter's precision and sensitivity across various lighting situations. An extensive analysis guarantees a robust evaluation and verification of the device's dependability in practical situations.

3.5.3 LED (4150K) Direct Measurement

3.5.3.1 Measurement Approach

With a precise color temperature of 4150K, the LED used in the accuracy experiment was carefully and smoothly incorporated into the color sensor assembly. As the primary light source for the experiment, this LED was essential in ensuring accurate color measurements by delivering steady, controlled illumination. The integration procedure made Accurate readings possible, which guaranteed a good working relationship between the color sensor and the LED.

A methodical strategy was adopted for the accuracy experiment, making direct measurements using RAL K7 color standards. This required bringing the prototype CyanoMeter's tip close to the color reference surface. To provide an isolated environment for accurate and dependable color readings, the purposeful decision of direct measurement was made to remove any potential impact from nearby light sources. This meticulous methodology preserved the experiment's integrity and improved the accuracy of the CyanoMeter's color detection abilities.

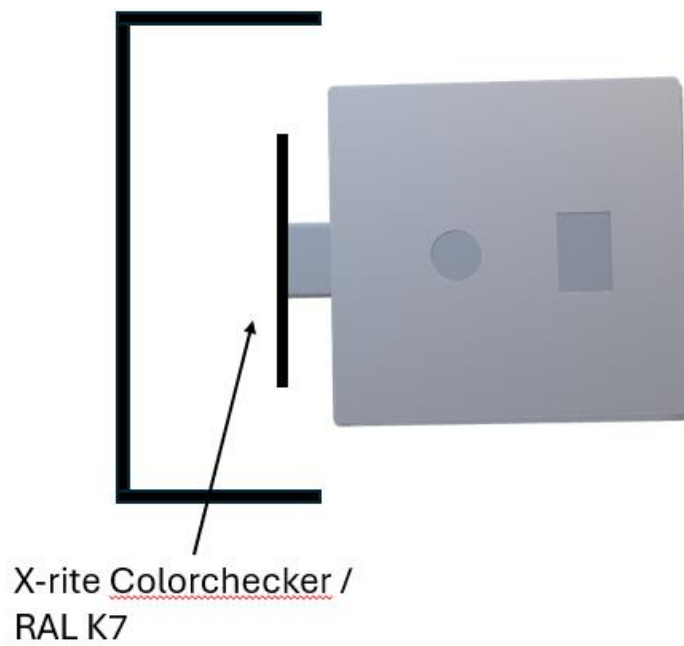


Figure 3.12: The illustration of measurement setup for LED (4150K) direct measurement



Figure 3.13: The direct measurement setup for LED (4150K)

3.5.3.2 Brightness Configuration

The ESP32 microcontroller was programmed to use pulse width modulation (PWM) to regulate the integrated LED's brightness. PWM is a method that regulates the amount of power supplied to a load, like an LED, using a sequence of pulses. The brightness of the LED can be adjusted by adjusting the average power given to the load, which is achieved by altering the pulse width.

With the CyanoMeter, for example, the LED brightness was calibrated to a precise value of 200, guaranteeing steady and regulated illumination throughout the readings. This purposeful decision was taken to prevent changes in LED brightness from affecting the device's functioning and potentially causing erroneous color measurements. The CyanoMeter is an effective instrument for identifying central cyanosis in infants since it can produce dependable and accurate results by keeping the LED brightness constant.

3.5.4 3000K Bulb and 6500K Bulb

3.5.4.1 Shared Measurement Setup

A standardized measurement setup was used for the 3000K and 6500K bulbs to guarantee experimental consistency. The RAL K7 color references, a collection of uniform color samples used in various industries, were lit by both lights. The CyanoMeter prototype's tip was positioned 5 cm away from the color references to create uniform conditions for evaluating the color sensor's accuracy in various illumination conditions.

The purpose of this deliberate inclusion of a range of lighting circumstances is to give a comprehensive and nuanced understanding of the accuracy and responsiveness of the CyanoMeter in various lighting scenarios. A thorough analysis like this

guarantees a reliable evaluation and validation of the device's dependability in practical uses. With its standardized measurement setup, the CyanoMeter helps identify central cyanosis in infants, yielding accurate and dependable results.

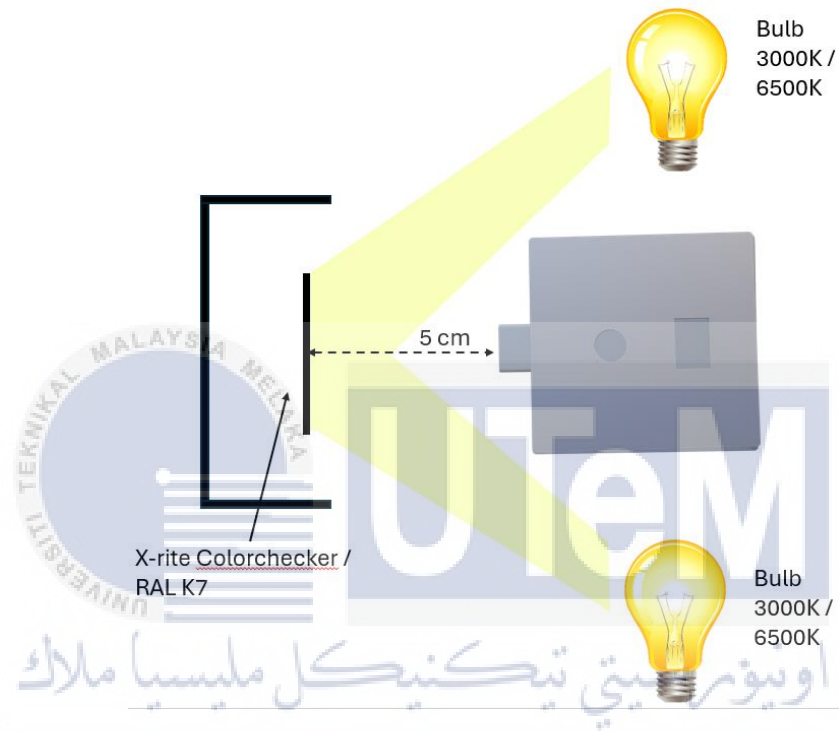


Figure 3.14: The illustration of measurement setup for bulb 3000K and 6500K

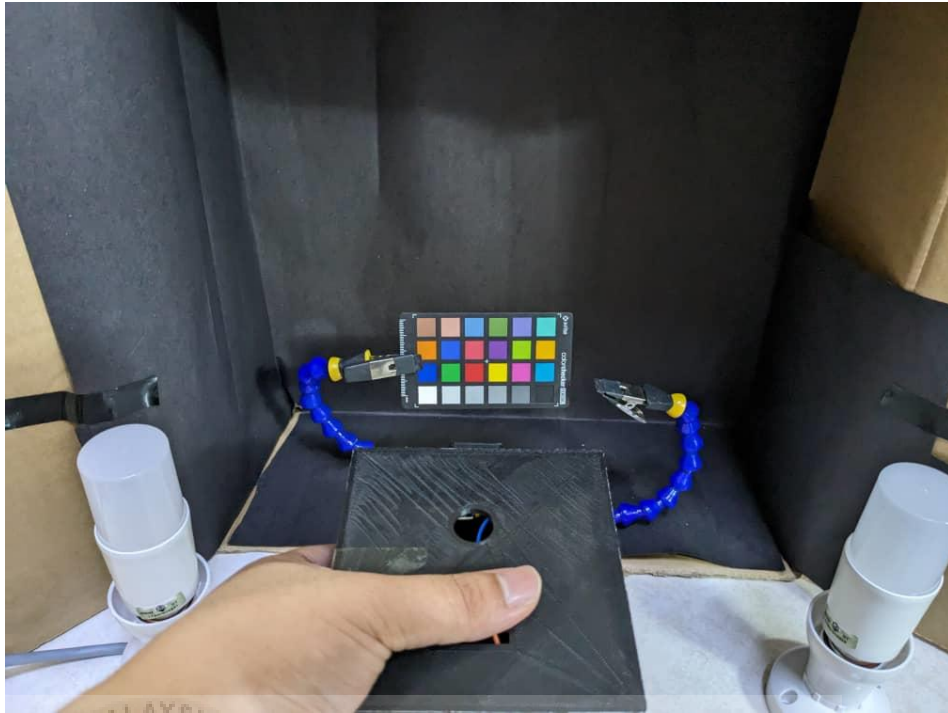


Figure 3.15: The measurement setup for bulb 3000K and 6500K

3.5.4.2 Distance Configuration

The CyanoMeter prototype and color reference were placed at a fixed distance of 5cm, which was selected to maximize color measurement accuracy under the distinctive illumination circumstances of the 3000K and 6500K bulbs. This distance parameter reduces the impact of outside light and other variables that can skew the measurements, ensuring that the color sensor on the CyanoMeter records accurate and trustworthy data.

3.6 IoT Implementation

The Blynk IoT system utilizes C++ libraries on the ESP32 microcontroller and cloud servers to enable customizable interfaces for real-time data visualization and notification triggers related to cyanosis. Sensor functions retrieve, process, and transmit RGB data from the ESP32 to the Blynk cloud, while time series graphs are used on the dashboard side to display color values. Blynk was purposefully chosen as

the IoT platform due to its adaptability and simplicity of integration, which offers a productive way to handle and monitor data in real time.

Blynk is used for more than just connectivity; it is a dynamic cloud-based archive for RGB color data that the CyanoMeter gathers. The Blynk program cleverly presents and visualizes this data, giving users an easy-to-use interface to obtain and understand the color information. The Blynk application's visual depiction of RGB color data is shown in Figure 3.16, providing a thorough and interactive view of the observed values.

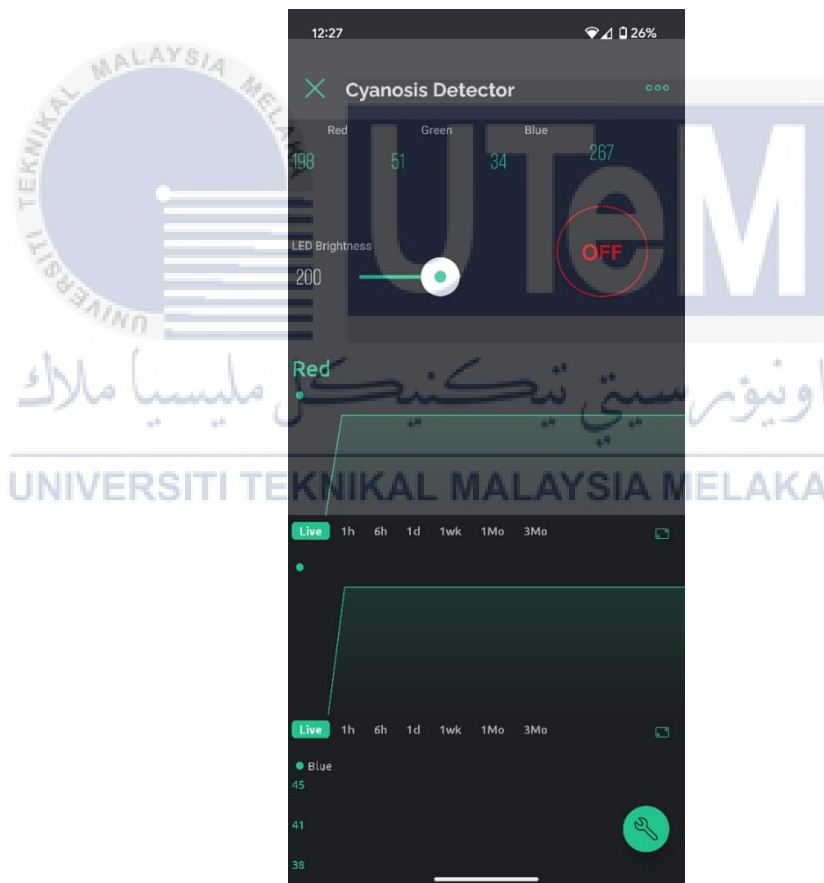


Figure 3.16: The Blynk's user interface for Cyanosis Detector

The smooth transfer of measurement data from the color sensor to the Blynk platform is vital to this integration. Through this bidirectional communication, the

CyanoMeter can continuously update the cloud-based platform with real-time color data and receive commands and instructions from the Blynk application. This dynamic data transmission method improves the CyanoMeter's monitoring capabilities, which also gives users fast and precise insights into color measurements.

3.7 Cyanosis RGB Threshold

Cyanosis in neonates presents a noticeable alteration in skin tone, particularly affecting the lips. In Caucasian infants with naturally lighter skin tones, cyanosis is characterized by a visible bluish hue on their lips. This change in color serves as an essential sign of underlying health issues. Specifically, the RGB values linked to cyanosis demonstrate consistently lower numerical values than those of non-cyanotic babies (see Table 3.5). This difference in RGB values provides a quantitative measure of the color variation related to cyanosis, offering valuable insights for detection and evaluation. The significance of these color-based indicators highlights the potential use of technological solutions, such as our proposed device, to improve the accuracy and effectiveness of detecting cyanosis in newborns.

Table 3.5: Cyanosis and non-cyanosis status

R	G	B	*L	*a	*b	Status
100	69	67	32.79	13.53	6.83	Cyanosis
129	86	77	41.23	17.5	12.89	Cyanosis
154	100	95	48.28	21.99	12.33	Cyanosis
143	96	85	45.7	18.66	14.48	Cyanosis
180	115	99	55.28	25	20.08	Non-Cyanosis
198	126	109	60.29	27.31	21.53	Non-Cyanosis
193	126	111	59.69	25.45	19.47	Non-Cyanosis
193	106	73	54.66	33.33	34.37	Non-Cyanosis

Significant RGB thresholds can be determined by examining the data in the Table 3.5, which are crucial for coding to guarantee precise identification of cyanosis within the system. Specifically, a threshold of less than 154 is established for the R channel. Simultaneously, the G channel must have a threshold of less than 100; for the B channel, it should be less than 95. Efficient detection of cyanosis depends on meeting these threshold requirements across all three channels. This criteria-driven approach forms an essential component of the coding framework, improving accuracy and dependability in identifying cyanosis within the system.

3.8 Color Measurement and Data Acquisition

3.8.1 Euclidean Distance in RGB

The color sensor of the CyanoMeter gathers RGB color values from the RAL K7 color card, which serves as a fundamental dataset for analysis. The Euclidean Distance formula is then utilized to evaluate the discrepancy between the measured RGB and anticipated theoretical values. The Euclidean Distance metric quantifies the correctness of color representation by measuring the distance between measured and theoretical values. Smaller distances indicate a closer alignment between the two. By employing this method, the CyanoMeter guarantees dependable and precise outcomes, rendering it an invaluable instrument for identifying central cyanosis in newborns. The formula is as follows:

$$\Delta E_{RGB} = \sqrt{(\Delta R)^2 + (\Delta G)^2 + (\Delta B)^2} \quad (3.1)$$

Each term ΔR , ΔG , and ΔB signifies the variation in intensity or value for the respective color channel. The square of each difference is computed and totaled, and subsequently, the square root of the total is derived. This procedure yields a solitary value, ΔE_{RGB} , which denotes the comprehensive distinction between two colors within

the RGB color space. A greater ΔE_{RGB} value suggests a more pronounced dissimilarity between these two colors.

3.8.2 T-test: Two-sample for Means

A T-test for means was used to assess the color sensor's precision even more. The statistical test involved comparing the theoretical RGB values and the means of the measured RGB values. As a statistical hypothesis test, the T-test for means is utilized to ascertain whether a significant difference exists between the means of two distinct groups. Applying the T-test for means to the CyanoMeter yielded significant findings regarding any substantial disparities between the measured and predicted RGB values, enhancing the overall evaluation of the color sensor's precision.

$$t = \frac{\bar{d}}{\frac{s_d}{\sqrt{n}}}$$

(3.2)

In this formula, t represents the t-statistic, a measure that indicates how far the sample mean difference (\bar{d}) deviates from the null hypothesis. The numerator, \bar{d} , signifies the average difference between the two groups being compared. Meanwhile, the denominator involves the standard deviation of these differences (s_d) divided by the square root of the sample size (\sqrt{n}). This standardization aids in adjusting for the influence of sample size on the variance in the data. The calculation of this ratio results in a t-statistic, which is then compared to critical values from a t-distribution to ascertain if the observed mean difference holds statistical significance. Essentially, this formula offers a quantitative evaluation of the probability that the noted disparity in means is not attributable to random chance but indicates an authentic differentiation between the groups.

3.8.3 Pearson Correlation Coefficient

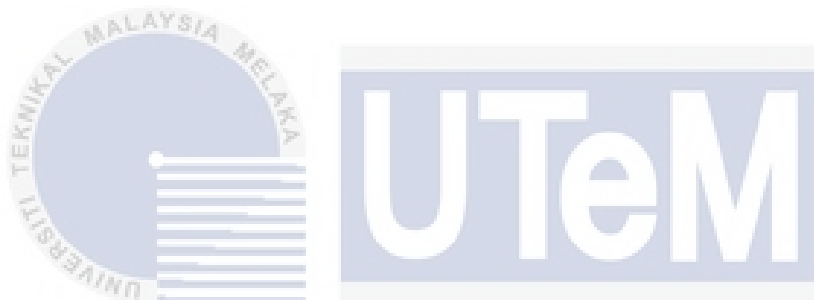
A statistical tool for determining the direction and intensity of the linear relationship between the measured and theoretical RGB values is the Pearson Correlation Coefficient. The accuracy of the color sensor in collecting color fluctuations is validated by the coefficient, which has a range of -1 to 1, with values near 1 suggesting a significant positive association. On the other hand, values around -1 would indicate an inverse correlation, while values near 0 would indicate no correlation.

$$r = \frac{\sum(x_i - \bar{x})(y_i - \bar{y})}{\sqrt{\sum(x_i - \bar{x})^2 \sum(y_i - \bar{y})^2}} \quad (3.3)$$



CHAPTER 4

RESULTS AND DISCUSSION



The following chapter details the outcomes of the experiment that was performed to assess the precision of the CyanoMeter's color sensor. The study aims to determine the accuracy of the color sensor by conducting a comparative analysis of the RGB values obtained from the actual and measured data. This study offers significant insights into the performance of the color sensor of the CyanoMeter, enhancing the evaluation of the device's dependability in practical scenarios.

4.1 LED (4150K) Direct Measurement

4.1.1 RAL K7 Color Reference Comparison and Euclidean Distance

The analysis begins by obtaining the measured values of the RAL K7 color reference under LED (4150K) setup. The average of the three measurements was compared to the RAL K7 standard RGB values. Statistical analyses were performed

in Microsoft Excel. The Dataset Lips were combined into one table to make it more systematic as there are some dataset lips that have shared the same RAL K7 color code. Table 4.1 shows the comparison values obtained from the measurement.

Table 4.1: RAL K7 color reference comparison between theoretical and measured with Euclidean distance for LED (4150K) direct measurements

Dataset Lip	Theoretical			Measured			Euclidean Distance
	R	G	B	R	G	B	
RAL 8007	112	69	42	110	62	36	9.43
RAL 8025	117	88	71	131	87	54	22.05
RAL 8024	121	80	56	128	78	47	11.58
RAL 8000	137	105	62	162	112	59	26.13
RAL 8004	141	73	49	173	72	48	32.03
RAL 8023	164	87	41	229	95	57	67.42
RAL 3016	166	61	47	218	60	48	52.02
RAL 1011	175	128	79	255	168	90	90.12
RAL 1024	186	143	76	255	200	96	91.71
RAL 3012	198	132	109	255	175	114	71.58
RAL 3022	207	105	85	255	133	99	57.31
AVERAGE							47.41

The LED (4150K) directly evaluates RGB values for different RAL K7 color standards, leading to several data points. RAL 8007 shows strong consistency between the anticipated and measured values, with minor discrepancies in each channel, indicating accurate color portrayal. Conversely, RAL 8025 displays significant variability across all channels, indicating a notable color deviation that warrants additional scrutiny. RAL 1024 stands out as having the highest Euclidean distance among all the color samples. The measured values in all three channels deviate significantly from the theoretical values.

The dataset's average Euclidean distance, which is 47.41, provides a comprehensive measure of the overall color accuracy of the device when measured

under an LED (4150K) light source. A lower average Euclidean distance indicates better alignment between theoretical and measured RGB values, demonstrating improved reliability in color detection. The consistent measurements across different RAL K7 color references support the device's ability to accurately capture color information under specific lighting conditions. Particularly, its reliable performance under LED (4150K) illumination highlights the suitability of this lighting scenario for obtaining precise color measurements and confirms the device's effectiveness in practical applications.

4.1.2 Statistical Analysis

Table 4.2: Statistical analysis for LED (4150K)

	R		G		B	
	<i>Theoretical</i>	<i>Measured</i>	<i>Theoretical</i>	<i>Measured</i>	<i>Theoretical</i>	<i>Measured</i>
Mean	156.7273	197.3636	97.36364	112.9091	65.18182	68
Variance	1105.218	3340.655	755.4545	2415.491	446.3636	700.8
Observations	11	11	11	11	11	11
Pearson Correlation	0.964929		0.988886		0.906855	
Hypothesized Mean Difference	0		0		0	
df	10		10		10	
t Stat	-4.96232		-2.30744		-0.8112	
P(T<=t) one-tail	0.000284		0.021849		0.218067	
t Critical one-tail	1.812461		1.812461		1.812461	
P(T<=t) two-tail	0.000568		0.043697		0.436135	
t Critical two-tail	2.228139		2.228139		2.228139	

The mean values estimated for the RGB channels when measuring the LED (4150K) provide useful insights into the average color reproduction of the CyanoMeter under this specific lighting condition. The expected mean for the red channel (R) is approximately 156.73, but the measured mean is 197.36, indicating an overestimation of the red component compared to theoretical values. Likewise, while the anticipated average in the green channel (G) is 97.36, it was measured at 112.91,

consistently showing an overestimated value compared to expectations. In contrast, although a deviation exists between theoretical and measured means in blue channel (B), these closely align, suggesting an accurate depiction of its component.

After thoroughly analyzing the differences, it is evident that the recorded RGB channels have higher values than expected. This implies a broader distribution of values in the dataset, indicating possible inconsistencies in the CyanoMeter's ability to accurately replicate colors under LED (4150K) lighting conditions.

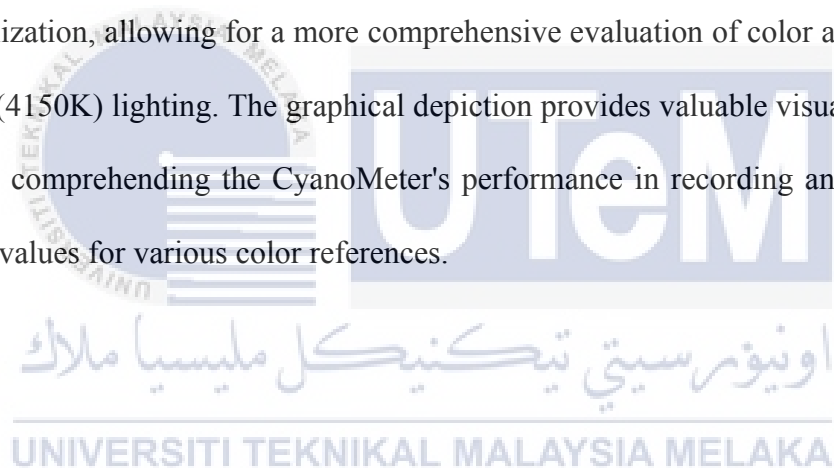
The negative t-statistics for all three channels (R, G, B) consistently indicate a disparity between the theoretical and measured averages. The p-values associated with these differences demonstrate their statistical significance, particularly for the red channel (p-value < 0.001), highlighting a strong bias. In summary, although the CyanoMeter may show small deviations from expected values in color reproduction under LED (4150K) lighting conditions for red, green, and blue channels, it still serves as a dependable tool for capturing color data. These minor inconsistencies do not significantly impact its overall functionality, and the CyanoMeter remains a valuable resource for evaluating color in clinical settings.

4.1.3 3D Scatter Plot Graph

RAL K7 color references' RGB values obtained through direct measurement with the LED (4150K) provide the basis for a 3D scatter plot graph generated with Python code. This graphic depiction is an effective analysis tool that thoroughly plots the measured and actual RGB values. The graph makes the differences between the two datasets easily visible, enabling a thorough examination of color changes.

The 3D scatter plot graph is created by the Python code using the matplotlib and mpl_toolkits.mplot3d packages. In the graph, each RAL K7 color reference is shown as a data point with coordinates that match the measured and actual RGB values. It is easy to identify trends and patterns in color differences by looking at the spatial distribution of these points. The plotted dots show the degree of color variation between the measured and actual RGB values if they are closely aligned. On the other hand, a significant divergence from the plot indicates noticeable differences in color representation.

The RGB information can now be better understood due to the 3D scatter plot visualization, allowing for a more comprehensive evaluation of color accuracy under LED (4150K) lighting. The graphical depiction provides valuable visual insights that aid in comprehending the CyanoMeter's performance in recording and reproducing RGB values for various color references.



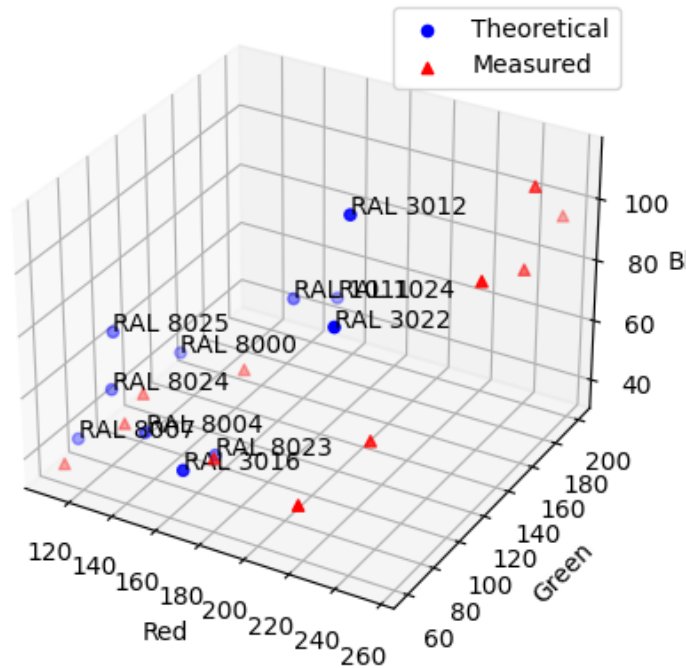


Figure 4.1: 3D scatter plot graph between theoretical and measured RGB values for LED (4150K) direct measurements

The graph, a three-dimensional scatter plot, shows the color coordinates for several color samples as Red, Green, and Blue (RGB) values. Red triangles indicate the measured values and blue dots represent the theoretical values. Every point has a unique RAL code written on it. For every RAL code, there are differences between the measured and theoretical values, showing that real-world measurements differ from the predicted theoretical values.

The graph indicates that, despite minor deviations, the measured RGB values are generally within a reasonable range of the theoretical values. For instance, the measured RGB values, especially in the green channel, for RAL 8000 are more significant than the theoretical values. On the other hand, RAL 8025's measured RGB values are less than its theoretical values, suggesting a notable color shift that needs more research.

4.1.4 Pearson Correlation Coefficient

Pearson Correlation Coefficient graph is generated using Python. The data was based on the findings using CyanoMeter. Figure 4.2 shows the Pearson Correlation Coefficient graph for all R, G, and B channels.

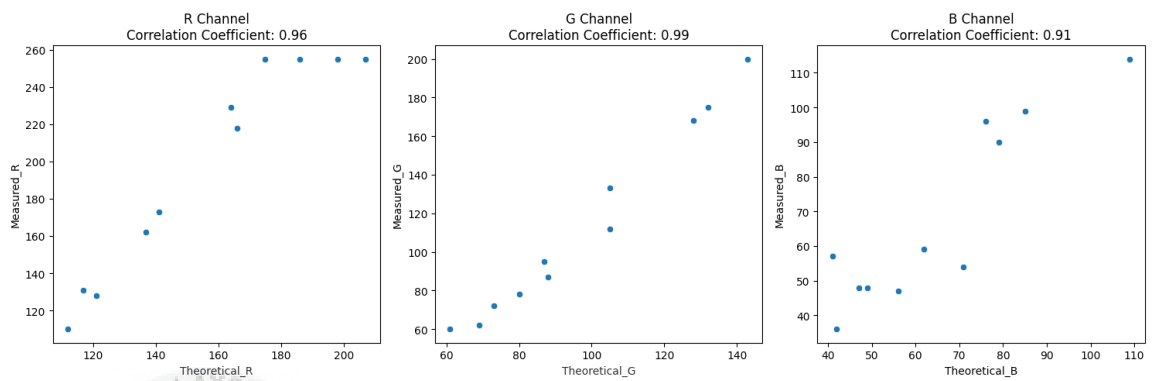


Figure 4.2: Pearson Correlation Coefficient graph on each RGB channels for LED (4150K) direct measurements

The Red channel has a substantial positive linear connection between the theoretical and measured red values, as indicated by the high correlation coefficient 0.96. These findings suggest that the CyanoMeter effectively reproduces red colors with constant accuracy when exposed to LED (4150K) lighting. The linear trend is statistically significant, highlighting the device's capacity to capture changes in the red component precisely.

A correlation coefficient 0.99 for the green channel indicates a highly significant positive linear relationship between the theoretical and measured green values. The CyanoMeter's exceptional precision in replicating green colors demonstrates its reliability and accuracy in capturing tiny nuances in the green component.

The blue channel exhibits a correlation coefficient of 0.91, indicating a robust positive connection, but significantly lower than that observed in the red and green channels. This shows a strong albeit slightly less accurate linear correlation between the theoretical and measured blue levels. The CyanoMeter exhibits proficiency in detecting fluctuations in the blue component; however, there may be potential for enhancing its precision.

The analysis of all three channels indicates a constant and robust positive linear correlation between the theoretical and measured RGB values. The consistency of the correlation coefficients indicates that the CyanoMeter reliably replicates colors when exposed to the required LED (4150K) lighting.

Although there are substantial correlations, the negative t-statistics and high p-values indicate the presence of systematic biases that result in overestimation, particularly in the red and green channels.

4.2 Bulb (3000K) Measurement

4.2.1 RAL K7 Color Reference Comparison and Euclidean Distance

The collected data was obtained using the measurement setup for Bulb 3000K and 6500K. In this experiment, two 3000K bulbs were used as the primary sources of warm white illumination for the whole measuring process. The purposeful choice of these particular bulbs was made to replicate warm indoor lighting settings, confirming the experiment's applicability to real-life situations.

Table 4.3: RAL K7 color reference comparison between theoretical and measured with Euclidean distance for bulb (3000K) measurements

Dataset Lip	Theoretical	Measured	
-------------	-------------	----------	--

	R	G	B	R	G	B	Euclidean Distance
RAL 8007	112	69	42	112	74	43	5.1
RAL 8025	117	88	71	117	76	46	27.73
RAL 8024	121	80	56	131	76	47	14.04
RAL 8000	137	105	62	150	106	62	13.04
RAL 8004	141	73	49	139	74	46	3.74
RAL 8023	164	87	41	169	89	54	14.07
RAL 3016	166	61	47	172	72	49	12.69
RAL 1011	175	128	79	191	116	59	28.28
RAL 1024	186	143	76	224	140	74	38.17
RAL 3012	198	132	109	210	102	63	56.21
RAL 3022	207	105	85	255	129	83	53.7
AVERAGE							21.31

After conducting a thorough analysis, it becomes evident that specific color references display significant inconsistencies between their theoretical and empirical RGB values. For example, the RAL 8007 exhibits a marginal Euclidean distance of 5.1, which signifies a substantial correspondence between the theoretical and measured RGB values. In contrast, RAL 3012 exhibits a significantly greater Euclidean distance of 56.21, indicating that the color representation varies more substantially.

Upon conducting a collective dataset analysis, an average Euclidean distance of 21.31 is calculated. This indicates it functions as a comprehensive metric for assessing the overall accuracy of colors, considering discrepancies among numerous color sources. A lower average Euclidean distance from the LED (4150K) configuration suggests that the CyanoMeter functions optimally when exposed to mild white light.

4.2.2 Statistical Analysis

Table 4.4: Statistical analysis for bulb (3000K) measurements

	R	G	B
--	---	---	---

	<i>Theoretical</i>	<i>Measured</i>	<i>Theoretical</i>	<i>Measured</i>	<i>Theoretical</i>	<i>Measured</i>
Mean	156.7273	170	97.36364	95.81818	65.18182	56.90909
Variance	1105.218	2124.2	755.4545	595.3636	446.3636	164.0909
Observations	11	11	11	11	11	11
Pearson Correlation	0.970812		0.864346		0.636345	
Hypothesized Mean Difference	0		0		0	
df	10		10		10	
t Stat	-2.75983		0.370424		1.682246	
P(T<=t) one-tail	0.010068		0.359396		0.061717	
t Critical one-tail	1.812461		1.812461		1.812461	
P(T<=t) two-tail	0.020136		0.718792		0.123434	
t Critical two-tail	2.228139		2.228139		2.228139	

The measurements and theoretical mean values for the RGB channels indicate the data's central tendency. For example, the theoretical mean for the red channel (R) is 156,7273; the corresponding measured mean is 170. Analogous correlations regarding the blue (B) and green (G) channels may be established. Varying degrees of dispersion from the mean variances indicate the extent to which the data points are dispersed. Observed in the red channel is a variance of 2124.2, which suggests that the measured values contain some degree of variation.

The t-test statistics assess whether the difference between the theoretical and measured means is statistically significant. A comparison is made between the t-statistics of each channel (R, G, B) and the critical t-values. The t-statistic for the red channel is -2.75983, which is less than the critical value and thus indicates that the difference is statistically significant. Nonetheless, the t-test shows that the distinctions between the green and blue channels are not statistically significant.

4.2.3 3D Scatter Plot Graph

The 3D scatter plot graph illustrates the relationship between the measured and theoretical RGB values, as shown in Figure 4.3. The graph visually represents the data

points in a three-dimensional space, showcasing the alignment or deviation between the expected and actual values for each color channel.

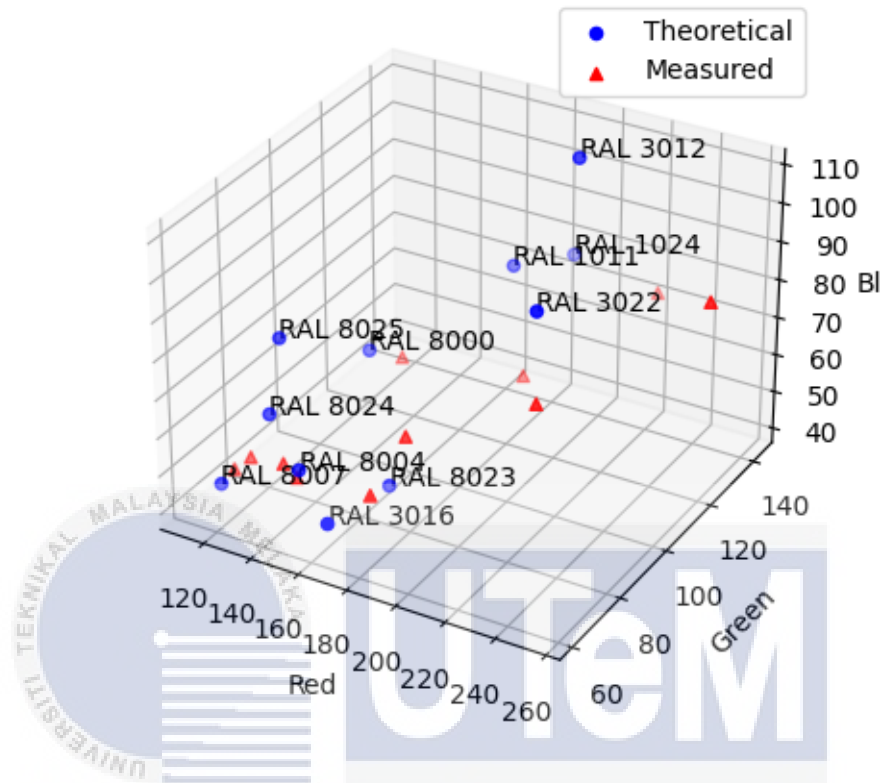


Figure 4.3: 3D scatter plot graph between theoretical and measured RGB values for bulb (3000K) measurements

The visual representation shown in Figure 4.3 demonstrates the strong correlation between the theoretical and observed RGB values. The plot demonstrates a strong and harmonious relationship, suggesting that the values are not significantly different. The visual depiction highlights the enduring and uniform color precision, contrasting the graph representing the LED (4150K) experiment.

The comparative inspection of the two plots reveals significant stability and decreased fluctuation in the RGB values when exposed to Bulb (3000K) lighting. The stability observed suggests a dependable and uniform color representation, as discrepancies between the anticipated and measured values are minimized. The graph

demonstrates the increased stability of the CyanoMeter when used under the specific illumination conditions provided by the Bulb (3000K). This indicates that the CyanoMeter is reliable for accurately assessing color in the defined environment.

4.2.4 Pearson Correlation Coefficient

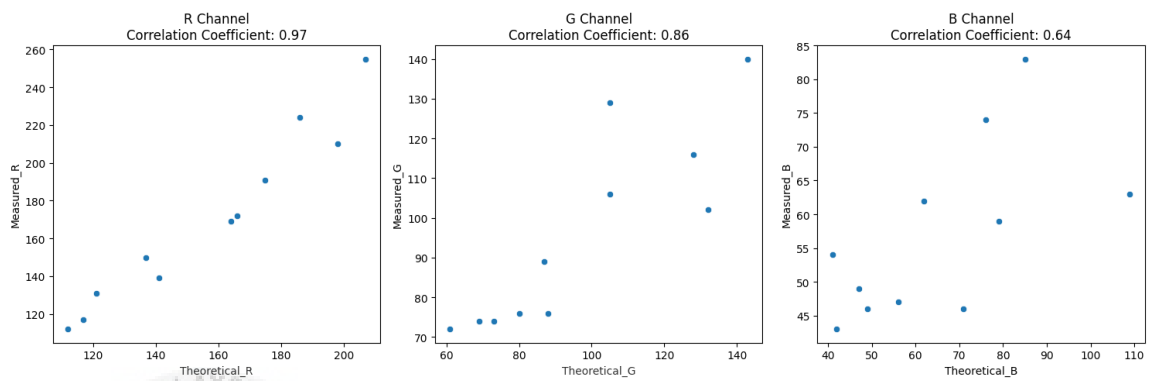


Figure 4.4: Pearson Correlation Coefficient graph on each RGB channels for bulb (3000K) measurement

Analyzing all three Pearson correlation coefficients for the RGB channels provides valuable insights into the performance of the CyanoMeter. The red channel exhibits a significantly high correlation coefficient of 0.97, indicating a strong and persistent linear link between the theoretical and measured values. This shows a consistent precision in detecting changes in the red color range. Transitioning to the green channel, the correlation coefficient of 0.86, while slightly lower than that of the red channel, nevertheless indicates a robust linear relationship. However, this shows a reliable measurement result in the green color range with slightly more variation compared to the red channel. The correlation coefficient of 0.64 in the blue channel suggests a less strong linear relationship when compared to both the red and green channels. Although the correlation remains positive, the decreased correlation implies some unpredictability or non-linearity when monitoring blue values.

After thoroughly analyzing the RGB values dataset acquired using Bulb 6500K, it is evident that there is a substantial variation in the Euclidean distance among several RAL K7 color standards. Consider, as an example, RAL 8007, which has theoretical RGB values of 112 (R), 69 (G), 42 (B), and observed values at Bulb 6500K of 119 (R), 151 (G), 128 (B). The Euclidean distance associated with RAL 8007 is significantly high, measuring 119.03. This indicates a substantial discrepancy between the expected and actual colors. The pattern remains consistent across different color references, displaying a range of Euclidean distances. Specific references exhibit a stronger correlation between the theoretical and measured values, whereas others display more significant discrepancies.

Examining the dataset thoroughly assesses the CyanoMeter's ability to measure color accurately under Bulb 6500K lighting. The calculated mean Euclidean distance among all references is a comprehensive measure for overall accuracy, considering variations across multiple color samples. The Bulb 6500K conditions exhibited the highest color error among the other two lighting conditions, with an average color error of 118.42.

4.3.2 Statistical Analysis

Table 4.6: Statistical analysis for bulb (6500K) measurements

	R		G		B	
	<i>Theoretical</i>	<i>Measured</i>	<i>Theoretical</i>	<i>Measured</i>	<i>Theoretical</i>	<i>Measured</i>
Mean	156.7273	159.9091	97.36364	179.3636	65.18182	149.9091
Variance	1105.218	1018.691	755.4545	686.4545	446.3636	247.6909
Observations	11	11	11	11	11	11
Pearson Correlation	0.995099		0.940741		0.811469	
Hypothesized Mean Difference	0		0		0	
df	10		10		10	
t Stat	-3.0258		-29.1575		-22.6136	
P(T<=t) one-tail	0.006384		2.63E-11		3.22E-10	

t Critical one-tail	1.812461	1.812461	1.812461
P(T<=t) two-tail	0.012768	5.25E-11	6.44E-10
t Critical two-tail	2.228139	2.228139	2.228139

The dataset representing RGB values under Bulb 6500K is characterized by notable variations in the theoretical and measured values across different color channels (R, G, B). The mean values provide an overview of the central tendencies, indicating the average theoretical and measured RGB values for the selected color references. For instance, the mean theoretical values are 156.7273 (R), 97.36364 (G), 65.18182 (B), while the mean measured values are 159.9091 (R), 179.3636 (G), 149.9091 (B).

The variance in the dataset signifies the degree of dispersion among the measured values from their respective theoretical counterparts. In this context, the variance is 1018.691 for the red channel, 686.4545 for the green channel, and 247.6909 for the blue channel. These values provide insights into the spread of data points around the mean, helping to assess the consistency and reliability of the measurements.

The Pearson correlation coefficients quantitatively measure the linear relationship between the theoretical and measured RGB values for each color channel. In this dataset, high correlation coefficients are noted for all channels: 0.995099 (R), 0.940741 (G), and 0.811469 (B). These values indicate strong positive linear relationships, suggesting that the theoretical and measured values move together predictably.

The t-statistic and associated p-values provide statistical significance tests for the mean differences between theoretical and measured values. For the red channel, the t-statistic is -3.0258, with a very low p-value of 0.006384, indicating a significant difference between the means. The t-statistics for the green and blue channels are even

more pronounced, being -29.1575 and -22.6136, respectively, with extremely low p-values. These results suggest that the differences between the theoretical and measured values are statistically significant.

4.3.3 3D Mapping Graph

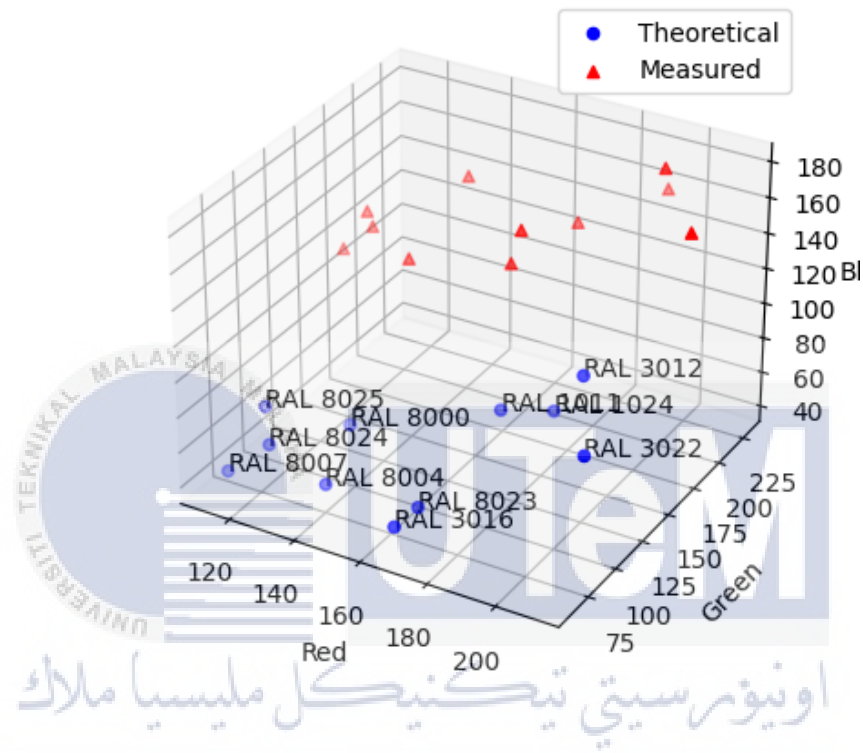


Figure 4.5: 3D scatter plot graph between theoretical and measured RGB values for bulb (6500K) measurements

A discernible trend becomes apparent when examining the RGB values under Bulb 6500K conditions in detail using the 3D mapping graph. Compared to the 3D mapping graphs produced under LED (4150K) and Bulb (3000K) circumstances, the plot between the measured and theoretical RGB values seems much more scattered. The Bulb 6500K graph's broad spread of data points suggests significant differences between theoretical and observed values, which may make it challenging to record color information in daylight precisely.

Compared to the other two lighting conditions, this dispersion is strongly emphasized. The arrangement of data points in the LED (4150K) and Bulb (3000K) graphs is more compact and closely packed, suggesting a higher degree of agreement between the CyanoMeter's readings and the predicted theoretical values. The noticeable discrepancy in the Bulb 6500K graph indicates that the CyanoMeter performs less accurately throughout the day.

To sum up, the 3D mapping graph visually depicts the CyanoMeter's effectiveness in various lighting scenarios. The Bulb 6500K graph's noticeable dispersion suggests color accuracy problems in daylight, emphasizing how important it is to select the best lighting conditions for the CyanoMeter to function.

4.3.4 Pearson Correlation Coefficient

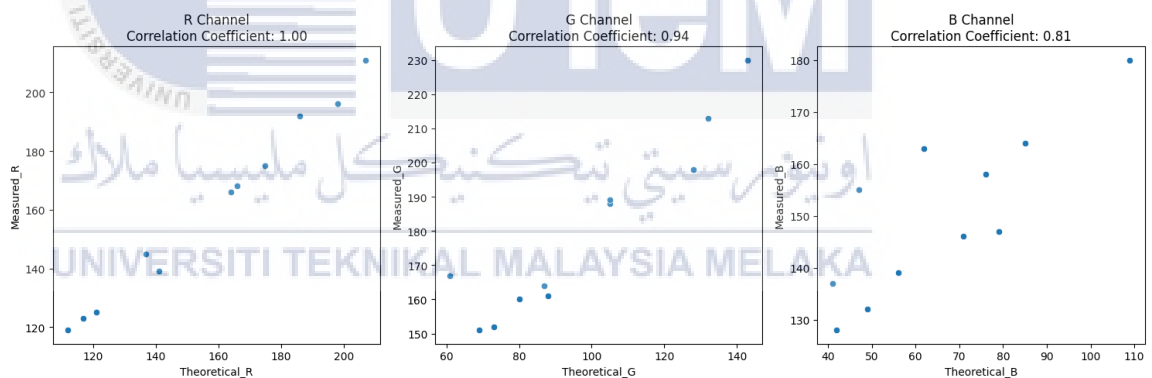


Figure 4.6: Pearson Correlation Coefficient graph on each RGB channels for bulb (6500K) measurement

With a value of 1.00, the Pearson correlation coefficient for the red channel is very strong. According to this perfect positive correlation, the measured and theoretical red color values have an exact linear connection. Strong performance in faithfully recording red hues is indicated by the strong correlation between the CyanoMeter's

measurements for the red channel under Bulb 6500K and the expected theoretical values.

There is a substantial positive correlation between the measured and theoretical green color levels, as indicated by the 0.94 Pearson correlation coefficient for the green channel. This score indicates a very strong correlation, even though the correlation is somewhat less than ideal. Under Bulb 6500K, the CyanoMeter consistently and accurately measures the green channel, confirming its efficacy in gathering data on green color.

The Blue channel's Pearson correlation coefficient is 0.81, which indicates a high positive connection marginally weaker than the red and green channels. This could suggest that, under Bulb 6500K settings, there is a comparatively higher variability or dispersion in the recorded blue color values. Even while the association is still strong, it suggests that caution and possibly some changes are necessary when examining blue color data collected under these lighting conditions.

In conclusion, under Bulb 6500K illumination, the CyanoMeter's precision and dependability in recording these color components are demonstrated by the strong correlation coefficients for the red and green channels. The blue channel's weaker correlation points to a subtle element that might need more research. These correlation values offer insightful information about how well the device works, helping to direct future adjustments for improved color accuracy in daylight.

4.4 Results Discussion

The examination of RGB values captured under different lighting conditions, specifically LED (4150K), Bulb (3000K), and Bulb (6500K), reveals interesting

patterns and variations in the CyanoMeter's ability to detect cyanosis. Upon analyzing the results, it is evident that LED illumination at 4150K and bulb illumination at 3000K offer the most optimal circumstances for precise cyanosis detection.

When subjected to LED (4150K) light, the CyanoMeter consistently displayed accurate readings with minimal Euclidean distances compared to various RAL K7 color references. The RGB values obtained under this lighting condition closely corresponded with theoretical values, highlighting the device's reliability and precision.

Similarly, under bulb (3000K) lighting, noteworthy results were observed with low Euclidean distances. The CyanoMeter consistently provided RGB values matching theoretical expectations when exposed to warm white light from a 3000k bulb. This indicates the device's exceptional performance in this specific lighting environment, reinforcing its trustworthiness for detecting cyanosis.

In contrast, measurements taken under bulb (6500K) illumination showed higher Euclidean distances, pointing towards relatively lower accuracy in capturing color information. These discrepancies between theoretical and measured RGB values imply potential challenges in accurately identifying cyanosis under this lighting scenario.

To summarize, LED (4150K) and bulb (3000K) lighting conditions emerge as highly favorable for effective performance detecting cyanosis. These observations underscore the importance of accounting for specific lighting conditions in the practical application of the device. LED and warm white bulb lighting not only

contribute toward precise measurements but also bolster the reliability of the CyanoMeter, a non-invasive tool for early detection of cyanosis in newborns.

4.5 Sustainability and Environmental Friendly

4.5.1 SDG 3: Good Health and Well-being

SDG 3 is supported by the project's contribution to non-invasive cyanosis detection. The advancement of a device that utilizes color sensors to quantify color values in the RGB space would facilitate the timely and effective identification of cyanosis, thereby fostering improved health outcomes and overall well-being.

4.5.2 SDG 9: Industry, Innovation, and Infrastructure

SDG 9 is aligned with integrating an Internet of Things (IoT) component within the initiative. Utilizing IoT to analyze color values facilitates technological advancements in the healthcare industry. In addition to improving infrastructure, this promotes developments that have the potential to enhance medical diagnostics.

4.5.3 SDG 10: Reduced Inequalities

The study reduces inequalities (SDG 10) by offering a non-intrusive and more readily available approach for detecting cyanosis. The availability of affordable and efficient early detection methods can help decrease health inequalities and guarantee that anyone, irrespective of their geographical location or financial situation, can obtain high-quality healthcare diagnostics.

4.5.4 SDG 17: Partnerships for the Goals

SDG 17 underscores the significance of cooperation and alliances. The project supports this objective by potentially facilitating partnerships among the healthcare industry, technology innovators, and other relevant parties. Interdisciplinary

collaboration is necessary to achieve the greater objective of enhancing health outcomes through the utilization of color sensors and IoT in healthcare.



CHAPTER 5

CONCLUSION AND FUTURE WORKS



5.1 Conclusion

In summary, the goal of this research was to develop a non-invasive device for detecting cyanosis by utilizing a color sensor to capture and analyze RGB color values. These values were then assessed through an Internet of Things setup. Both objectives were successfully achieved through thorough experimentation and analysis. The resulting CyanoMeter appears as a promising tool for non-invasive identification of cyanosis, thus representing a valuable contribution to healthcare technology.

Examining color values across different illumination conditions yielded significant findings regarding the device's performance. Significantly, the LED (4150K) and Bulb (3000K) temperatures proved to be the most dependable when employing a CyanoMeter. Showcasing its potential for practical implementations, the device

exhibited enhanced accuracy and precision while operating under these conditions. Implementing a moderate illumination bulb (3000K) and selecting the LED (4150K) condition, which served as a standardized lighting source, were critical factors in attaining consistent and dependable color measurements.

The CyanoMeter project accomplishes its primary goals and establishes a foundation for continuous progress in non-invasive medical technology. The accomplishment of key milestones and the identification of forthcoming endeavors highlight the project's importance in tackling critical healthcare challenges. The research outcomes and advancements presented in this study establish a solid basis for further investigation, guaranteeing the CyanoMeter's ongoing significance and influence within the ever-evolving domain of healthcare technology.

5.2 Future Works

5.2.1 Exploration of Advanced Color Sensors for Enhanced Precision

The upcoming focus of the CyanoMeter project will involve delving into advanced color sensor technologies to improve the precision of color measurements. This initiative is geared towards boosting the device's diagnostic capabilities and overall effectiveness by exploring state-of-the-art sensors that prioritize exceptional precision for cyanosis detection.

An in-depth assessment of cutting-edge color sensors currently available in the market is being conducted with a specific goal: to carefully select or develop sensors that offer enhanced sensitivity, resolution, and spectral accuracy. Besides hardware upgrades, incorporating sophisticated sensors will require developing custom algorithms and calibration methods to enhance the CyanoMeter's color measurement capabilities.

The research team anticipates that their exploration of advanced color sensors will establish new standards in non-invasive medical diagnostics. Their progressive approach underscores a commitment to continuous improvement and innovation, ensuring that the CyanoMeter remains a pioneering instrument in color-based medical diagnostics.

5.2.2 Real Patient Analysis

This segment represents the key transition from controlled laboratory settings to real-world healthcare environments. In this section, the CyanoMeter is validated in authentic patient environments to ensure that it is capable of accurately identifying cyanosis in a wide range of individuals. The primary objective is to establish a connection between controlled environments and clinical practicability, thereby preparing the groundwork for the integration of the CyanoMeter into standard patient care. During this stage, healthcare professionals and diverse patient populations collaborate to demonstrate the device's dependability under real-life medical conditions.

5.2.3 Integration of Machine Learning Algorithms

The purpose of incorporating machine learning algorithms into the CyanoMeter is not simply to enhance technology, but rather to intentionally improve the accuracy of diagnostics. Through the utilization of these algorithms, the apparatus acquires the capability to detect subtle variations in color and patterns that may elude traditional analytical techniques. By employing this adaptive methodology, the CyanoMeter consistently enhances its comprehension of color data, enabling it to adjust to a wide range of patient profiles and developing medical knowledge.

It is expected that the incorporation of machine learning will serve as a fundamental aspect in the development of the CyanoMeter, promoting a dynamic and intelligent system that corresponds to the continuously growing field of medical diagnostics. By moving in this future direction, not only can the device's existing functionalities be improved, but also entirely new realms of cyanosis detection and analysis may be unlocked.

5.2.4 Addition of Camera Module and Notification System

Integrating a camera module and a notification system into the CyanoMeter significantly advances the device's capabilities. This improvement aims to expand its functionalities beyond color sensor measurements, allowing for the acquisition of visual data to enhance the evaluation of skin color variations associated with cyanosis.

The ability to capture high-resolution images through an integrated camera module enables a detailed examination of skin color patterns. The expanded visual dataset provides supplementary contextual information that enhances the accuracy of color sensor measurements and contributes to a comprehensive assessment of cyanosis.

Additionally, the proposed notification system is designed to optimize the dissemination of diagnostic outcomes by providing healthcare professionals with prompt alerts if cyanosis is detected. This ensures efficient and effective responses, bridging communication between the CyanoMeter and medical professionals for accelerated intervention and improved patient outcomes.

Overall, integrating these features represents a paradigm shift, positioning the CyanoMeter as an intricate and versatile diagnostic instrument aligned with its

objective: facilitating effective communication and precise cyanosis detection in healthcare settings.



REFERENCES

- [1] S. K. Gupta, "Clinical Approach to a Neonate with Cyanosis," *The Indian Journal of Pediatrics*, vol. 82, no. 11, pp. 1050–1060, Nov. 2015, doi: 10.1007/s12098-015-1871-7.
- [2] S. Menahem, "Doctor the baby is blue! an approach to the diagnosis and management," *Int J Pregn & Chi Birth*, vol. 3, no. 1, pp. 203–207, 2017.
- [3] Y. A. Ali, H. K. Nossir, A. A. Nour, M. M. Baraka, N. M. Gamal, and M. H. El Sayed, "Transcatheter Closure of Right Pulmonary Artery to Left Atrium Fistula Under Transesophageal Echocardiography Guidance (a Case Report)," *SN Compr Clin Med*, vol. 2, no. 4, pp. 458–463, Apr. 2020, doi: 10.1007/s42399-020-00263-7.
- [4] J. Y. Lee, "Clinical presentations of critical cardiac defects in the newborn: Decision making and initial management," *Korean J Pediatr*, vol. 53, no. 6, p. 669, 2010, doi: 10.3345/kjp.2010.53.6.669.

- [5] S. Ghotra, K. Jangaard, C. Pambrun, and C. V. Fernandez, "Congenital methemoglobinaemia due to Hb F-M-Fort Ripley in a preterm newborn," *BMJ Case Rep*, p. bcr2016214381, Mar. 2016, doi: 10.1136/bcr-2016-214381.
- [6] C. Dani, L. Drovandi, G. Bertini, C. Poggi, and S. Pratesi, "Unexpected episodes of cyanosis in late preterm and term neonates prompted admission to a neonatal care unit," *Ital J Pediatr*, vol. 43, no. 1, p. 35, Dec. 2017, doi: 10.1186/s13052-017-0349-9.
- [7] L. E. Ellis and J. A. Beckman, "Baby blue," *Vascular Medicine*, vol. 19, no. 3, p. 215, 2014.
- [8] O. Anton *et al.*, "Non-invasive sensor methods used in monitoring newborn babies after birth, a clinical perspective," *Matern Health Neonatol Perinatol*, vol. 8, no. 1, p. 9, Nov. 2022, doi: 10.1186/s40748-022-00144-y.
- [9] J. W. Severinghaus, "Monitoring oxygenation," *J Clin Monit Comput*, vol. 25, no. 3, pp. 155–161, Jun. 2011, doi: 10.1007/s10877-011-9284-2.
- [10] L. Martin and H. Khalil, "How Much Reduced Hemoglobin Is Necessary to Generate Central Cyanosis?," *Chest*, vol. 97, no. 1, pp. 182–185, Jan. 1990, doi: 10.1378/chest.97.1.182.
- [11] A. Alakhfash, A. Alqwaiee, A. Almesned, and Z. N. Al-Hassnan, "Pulmonary arteriovenous malformation with unexplained cyanosis as the first presentation of hereditary haemorrhagic telangiectasia, case report, and literature review," *Eur Heart J Case Rep*, vol. 5, no. 7, Jul. 2021, doi: 10.1093/ehjcr/ytab261.

- [12] Y. Ling, T. Li, and Q. An, "Infant With Cyanosis," *Ann Emerg Med*, vol. 80, no. 2, pp. e17–e18, Aug. 2022, doi: 10.1016/j.annemergmed.2022.02.020.
- [13] C. Shin, M. Hong, M. Kim, and J. H. Lee, "Exon sequencing of the alpha-2-globin gene for the differential diagnosis of central cyanosis in newborns: a case report," *BMC Pediatr*, vol. 19, no. 1, p. 221, Dec. 2019, doi: 10.1186/s12887-019-1601-9.
- [14] M.-L. Laskine-Holland *et al.*, "The Association Between Cyanosis and Thromboelastometry (ROTEM) in Children With Congenital Heart Defects: A Retrospective Cohort Study," *Anesth Analg*, vol. 124, no. 1, pp. 23–29, Jan. 2017, doi: 10.1213/ANE.0000000000001708.
- [15] R. Cordina, S. Grieve, M. Barnett, J. Lagopoulos, N. Malitz, and D. S. Celermajer, "Brain volumetrics, regional cortical thickness and radiographic findings in adults with cyanotic congenital heart disease," *Neuroimage Clin*, vol. 4, pp. 319–325, 2014.
- [16] R. McNamara, C. M. Taylor, D. K. McKenzie, M. T. Coroneo, and S. J. Dain, "Colour change in cyanosis and the confusions of congenital colour vision deficient observers," *Ophthalmic and Physiological Optics*, vol. 30, no. 5, pp. 699–704, Sep. 2010, doi: 10.1111/j.1475-1313.2010.00752.x.
- [17] M. F. Ahmed and I. Kamel, "Apgar Scoring," in *Advanced Anesthesia Review*, A. Abd-Elsayed, Ed., Oxford University Press New York, 2023, pp. 817–C325.S9. doi: 10.1093/med/9780197584521.003.0324.

- [18] L. Lin *et al.*, “Apgar scores correlate with survival rate at discharge in extremely preterm infants with gestational age of 25-27 weeks,” *Brazilian Journal of Medical and Biological Research*, vol. 55, 2022, doi: 10.1590/1414-431x2022e12403.
- [19] A. Te Pas and R. Witlox, “Apgar score: time to call it?”, *Ned Tijdschr Geneeskd*, vol. 167, pp. D7321–D7321, 2023.
- [20] H. J. Rozycki and M. Yitayew, “The Apgar score in clinical research: for what, how and by whom it is used,” *J Perinat Med*, vol. 51, no. 4, pp. 580–585, May 2023, doi: 10.1515/jpm-2022-0340.
- [21] D. Blake, “Do we assess ‘colour’ appropriately using the Apgar score?,” *Journal of Neonatal Nursing*, vol. 16, no. 4, pp. 184–187, Aug. 2010, doi: 10.1016/j.jnn.2010.03.002.
- [22] A. Zeileis *et al.*, “colorspace: A Toolbox for Manipulating and Assessing Colors and Palettes,” *J Stat Softw*, vol. 96, no. 1, 2020, doi: 10.18637/jss.v096.i01.
- [23] Q. Chen, W. Liu, H. Wen, K. Liu, M. Chen, and J. Ma, “An enhanced 2-D color space diversity using RGB-LED overlapping for optical camera communication,” *Opt Commun*, vol. 545, p. 129636, Oct. 2023, doi: 10.1016/j.optcom.2023.129636.
- [24] N. F. B. Azmi, F. Delbressine, L. Feijs, and S. B. Oetomo, “Color Correction of Baby Images for Cyanosis Detection,” 2018, pp. 354–370. doi: 10.1007/978-3-319-95921-4_33.

- [25] M. Changizi and K. Rio, "Harnessing color vision for visual oximetry in central cyanosis," *Med Hypotheses*, vol. 74, no. 1, pp. 87–91, Jan. 2010, doi: 10.1016/j.mehy.2009.07.045.
- [26] G. Koch, "The Color Sensor," 2023, pp. 333–383. doi: 10.1007/978-1-4842-9280-8_9.
- [27] G. de Carvalho Oliveira, C. C. S. Machado, D. K. Inácio, J. F. da Silveira Petrucci, and S. G. Silva, "RGB color sensor for colorimetric determinations: Evaluation and quantitative analysis of colored liquid samples," *Talanta*, vol. 241, p. 123244, May 2022, doi: 10.1016/j.talanta.2022.123244.
- [28] A. Beyaz, "Comparison of Arduino Based Inexpensive Colormeters Effectiveness at Some Agricultural Products," *Fresenius Environ Bull*, vol. 26, pp. 6457–6469, Nov. 2017.
- [29] V. S. Siu *et al.*, "Toward a Quantitative Colorimeter for Point-of-Care Nitrite Detection," *ACS Omega*, vol. 7, no. 13, pp. 11126–11134, Apr. 2022, doi: 10.1021/acsomega.1c07205.
- [30] S. Prabowo, C. K. Utama Sutrisno, K. Purnawan Candra, A. Rahmadi, and Y. Yuliani, "Colorimeter design for dry food-products inspection using TCS3200 sensor and Arduino Mega-2560," *Advances in Food Science, Sustainable Agriculture and Agroindustrial Engineering*, vol. 6, no. 2, pp. 134–141, Jun. 2023, doi: 10.21776/ub.afssae.2023.006.02.4.
- [31] Yulkifli, P. Kahar, R. Ramli, S. B. Etika, and C. Imawan, "Development of color detector using colorimetry system with photodiode sensor for food dye

- determination application,” *J Phys Conf Ser*, vol. 1185, p. 012031, Apr. 2019, doi: 10.1088/1742-6596/1185/1/012031.
- [32] H. Singh, G. Singh, D. K. Mahajan, N. Kaur, and N. Singh, “A low-cost device for rapid ‘color to concentration’ quantification of cyanide in real samples using paper-based sensing chip,” *Sens Actuators B Chem*, vol. 322, p. 128622, Nov. 2020, doi: 10.1016/j.snb.2020.128622.
- [33] L. Chen, F. J. Ye, Y. Ruan, M. Cuo, S. S. Luo, and H. Y. Cui, “Trichromatic-color-sensing metasurface with reprogrammable electromagnetic functions,” *Opt Mater (Amst)*, vol. 123, p. 111892, Jan. 2022, doi: 10.1016/j.optmat.2021.111892.
- [34] A. Bima, S. Hadi, M. N. Fadli, N. Hidayah, and L. D. P. Arzani, “Designing a Honey Quality Tool Based on Gas Sensor and Color Sensor,” *International Journal of Engineering and Computer Science Applications (IJECSA)*, vol. 1, no. 2, pp. 94–102, Sep. 2022, doi: 10.30812/ijeCSA.v1i2.2407.
- [35] K. Todorova, D. Pavlov, and V. Petrov, “Uncertainty Budget for Calibration of Sensors for Measurement of Correlated Color Temperature,” in *2022 14th Electrical Engineering Faculty Conference (BulEF)*, IEEE, Sep. 2022, pp. 1–4. doi: 10.1109/BulEF56479.2022.10021184.
- [36] M. A. H. M. Adib, M. H. A. Rahim, I. M. Sahat, and N. H. M. Hasni, “Pediatrics Technology Applications: Enhance the Bilirubin Jaundice (BiliDice) Device for Neonates Using Color Sensor,” 2022, pp. 839–847. doi: 10.1007/978-981-33-4597-3_75.

- [37] “Color Converter.” [Online]. Available: <https://www.nixsensor.com/free-color-converter/>

